

NAPSUGARAS MAGSUGARAK



FRIB

Appalachian
STATE UNIVERSITY

Takács Endre

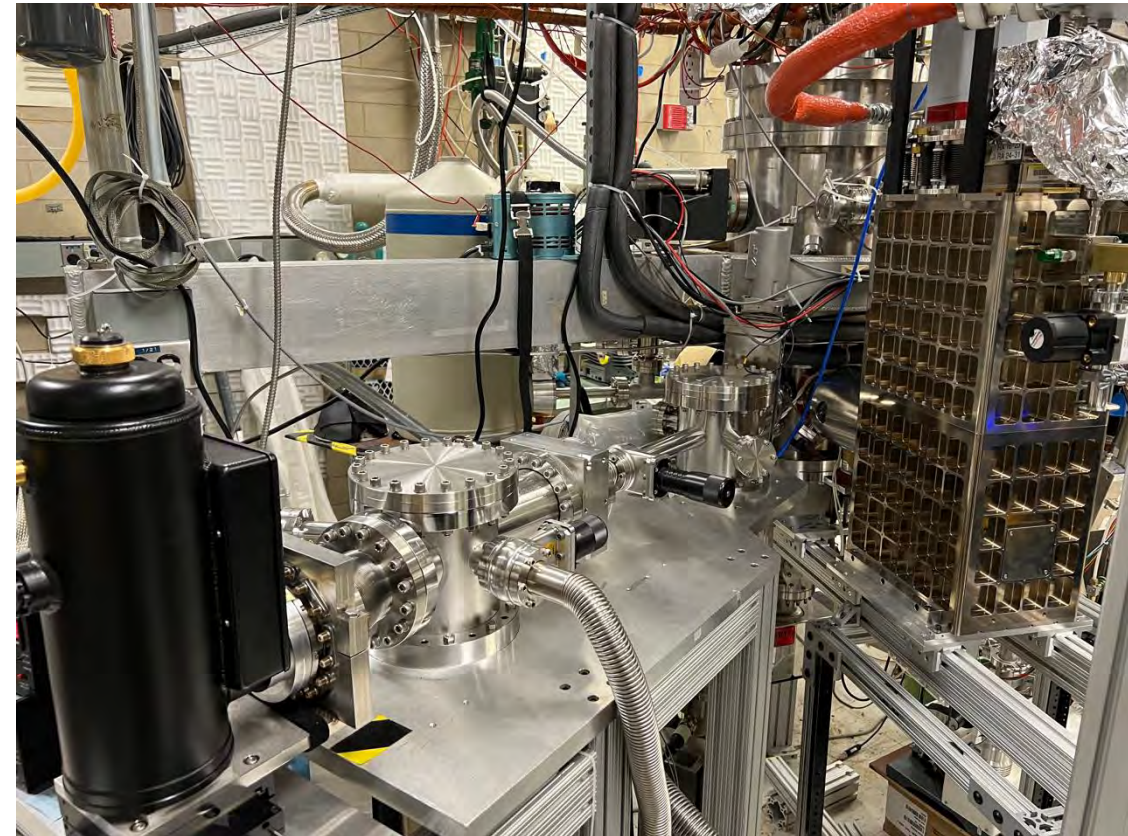
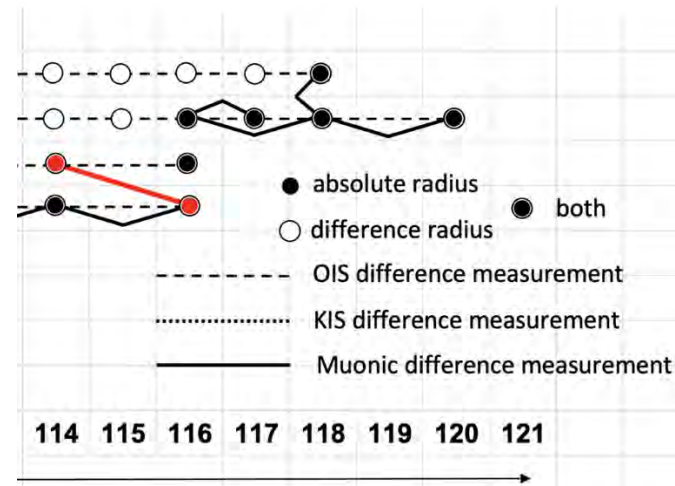
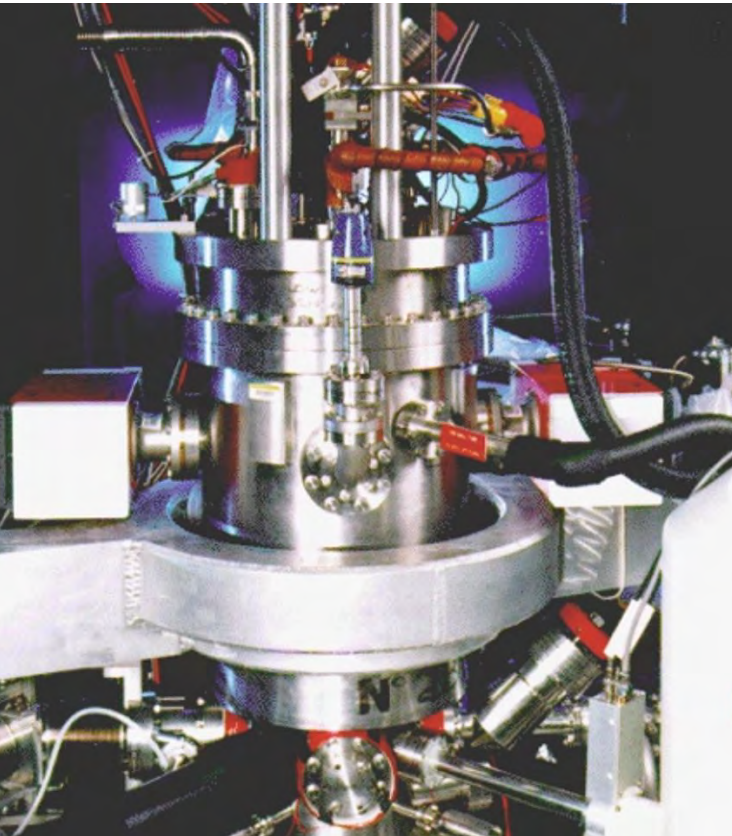
Clemson Egyetem, Dél-Karolina, USA



Hunter Staiger, Steven Blundell, Dipti, Gerald Gwinner, Roshani Silwal, Alain Lapierre,
John Gillaspay, Galen O'Neil, Joseph Tan, Yuri Ralchenko, Istvan Angeli



UNIVERSITY
OF MANITOBA



NEMZETKÖZI ATOMENERGIAI ÜGYNÖKSÉG (IAEA)



2025. január 27-30.



Clemson, Dél-Karolina



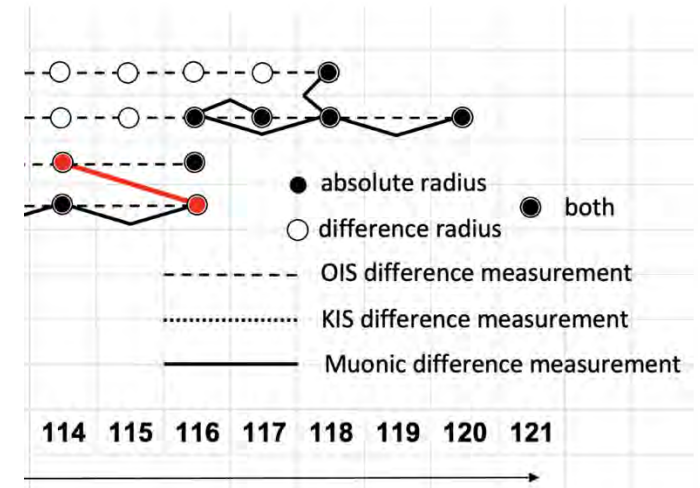
America's Best Small College Town Goes Big on School Spirit in a Tiny Corner of Upstate South Carolina

Clemson, South Carolina — home of Clemson University — has a growing downtown with a new hotel championing inclusivity.



VÁZLAT

- Magamról
- Motiváció újfajta atommag-töltéssugár mérésekre
- Nagytöltésű ionok
- Elektronnyaláb ioncsapda történet
- Nagytöltésű ionok spektroszkópiája
 - EUV, X-ray
- Atommag-töltéssugár felület
- Nagytöltésű ionokkal végzett töltéssugár mérések
 - Korábbi módszerek
 - Atommag-töltéssugár különbségek – Na-szerű ionok
 - Abszolút atommag-töltéssugarak – Na-szerű ionok
- Elemek közötti kényszerek
- További lehetőségek



MAGAMRÓL

- 1983-1989: Fizikus hallgató, Kossuth Lajos Tudományegyetem, Debrecen (témavezető: Angeli István)
- 1989 -1992: Ph.D. ösztöndíj, ATOMKI - Debreceni Egyetem (témavezetők: Ricz Sándor és Sulik Béla)
- 1992-1993: Soros post-doc ösztöndíj, Oxford University, Anglia
- 1993-1995: Postdoc állás, NIST, Washington, DC, USA
-
- 1995-1996: Magyar Zoltán Posztdoktori Ösztöndíj, Kísérleti Fizikai Tanszék, DE
- 1996-1999: Egyetemi Adjunktus, Kísérleti Fizikai Tanszék, DE, Kutató MTA-ATOMKI
- 1999-2001: Vendégkutató, MIT-NIST, Washington, DC, USA
- 2001-2012: Egyetemi Adjunktus, Kísérleti Fizikai Tanszék, DE
- 2012-2013: Egyetemi Docens, Kísérleti Fizikai Tanszék, DE
-
- 2013-2018: Associate Professor, Clemson Egyetem, Dél-Karolina, Vendégkutató NIST, Washington, DC, USA
- 2019 - Professor, Clemson Egyetem, Dél-Karolina, Vendégkutató NIST, Washington, DC, USA
- 2024-2025: Alkotói év, Harvard-Smithsonian Center for Astrophysics, National Institute for Fusion Science, Japan



MOTIVÁCIÓ ÚJFAJTA ATOMMAG-TÖLTÉSSUGÁR MÉRÉSEKRE



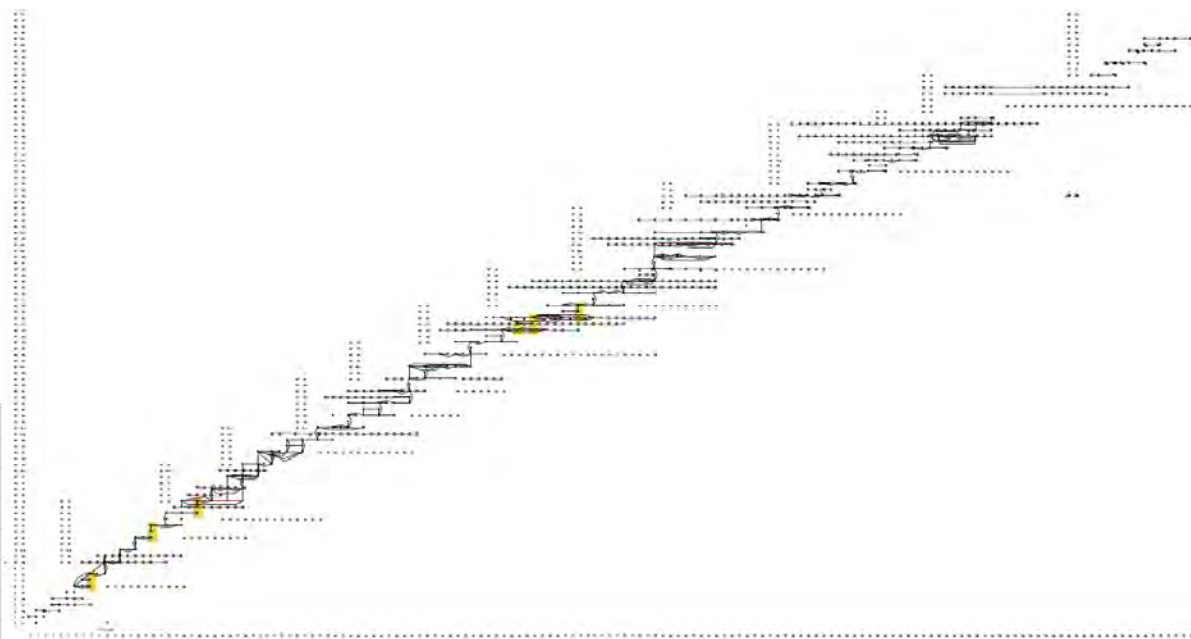
Atomic Data and Nuclear Data Tables

Volume 99, Issue 1, January 2013, Pages 69-95



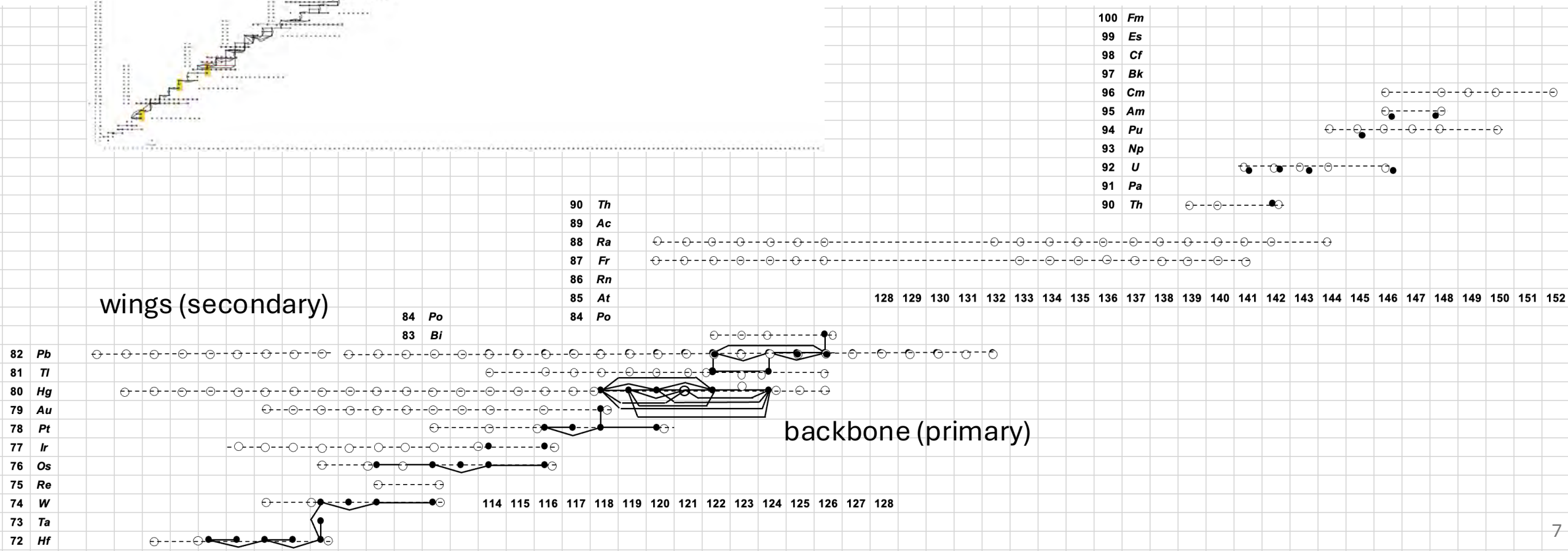
Table of experimental nuclear ground state charge radii: An update

I. Angeli ^a, K.P. Marinova ^b



wings (secondary)

backbone (primary)



TÖLTÉSSUGÁR ÉS ALAPVETŐ SZIMMETRIA TESZTEK

- ❖ Francium and radium are candidates in searches for physics beyond the Standard Model:
 - Ra-225: Permanent Electric Dipole Moments (EDM)
 - Fr: Atomic Parity Non-Conservation (APNC)
- ❖ The absolute charge radii of Fr and Ra were never directly measured.
- ❖ The absolute charge radius of Fr in the literature is obtained from extrapolations.
- ❖ **Need to determine absolute charge radius.**

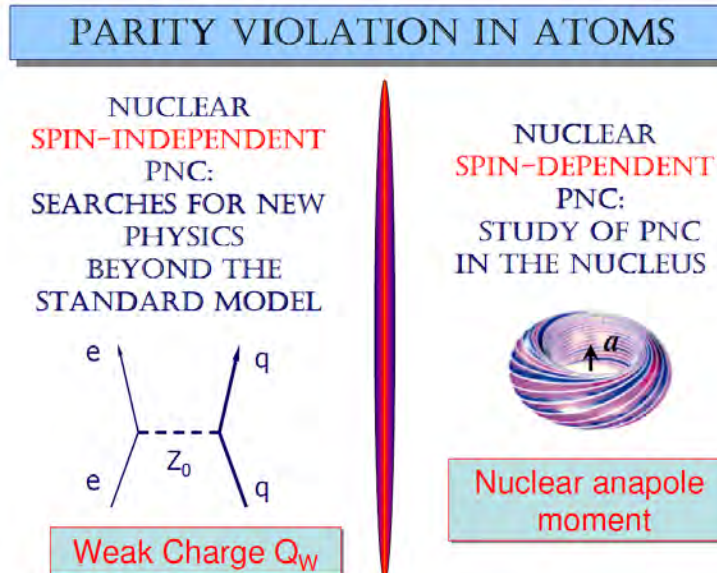
Why is it important ?

Atomic matrix element

$$H^{(1)} = \frac{G}{2\sqrt{2}} \gamma_5 Q_W \rho(r)$$

Weak coupling constant for symmetry tests

Charge density distribution



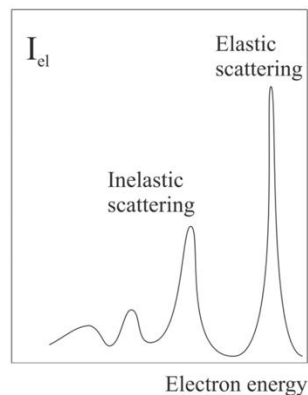
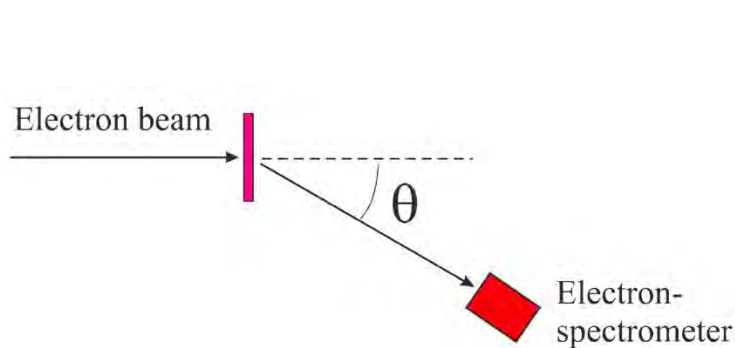
Atomic matrix element

$$H^{(2)} = \frac{G}{\sqrt{2}} \kappa_2 \alpha \cdot \mathbf{I} \rho(r)$$

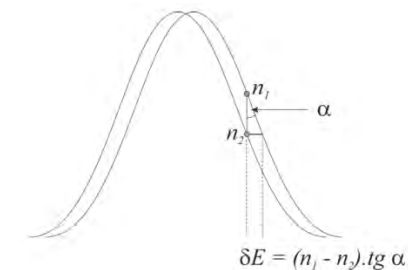
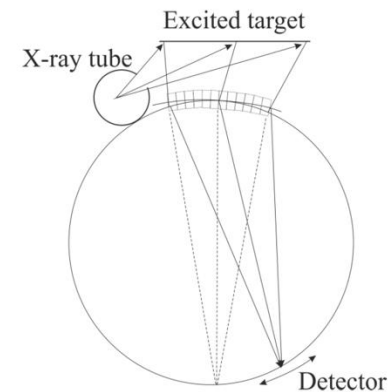
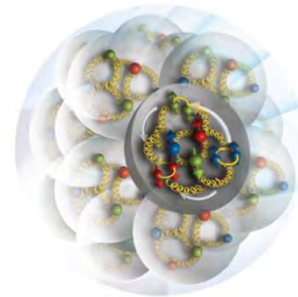
Nuclear spin

Charge density distribution

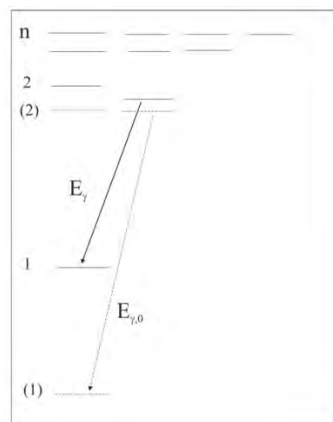
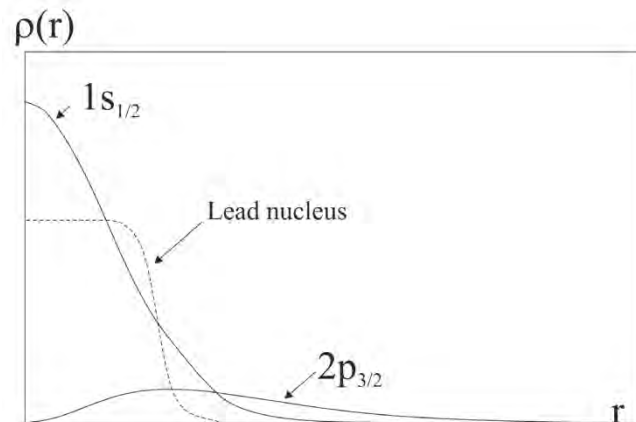
KLASSZIKUS ATOMMAG TÖLTÉSSUGÁR MÉRÉSEK



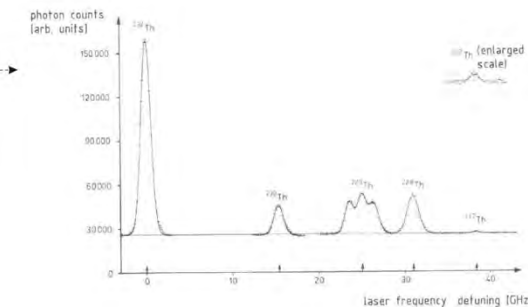
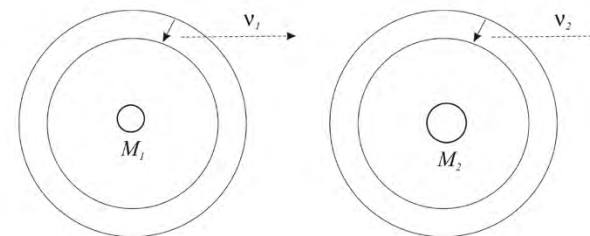
1. Elastic electron scattering



3. $K\alpha$ isotope shift of neutral atoms



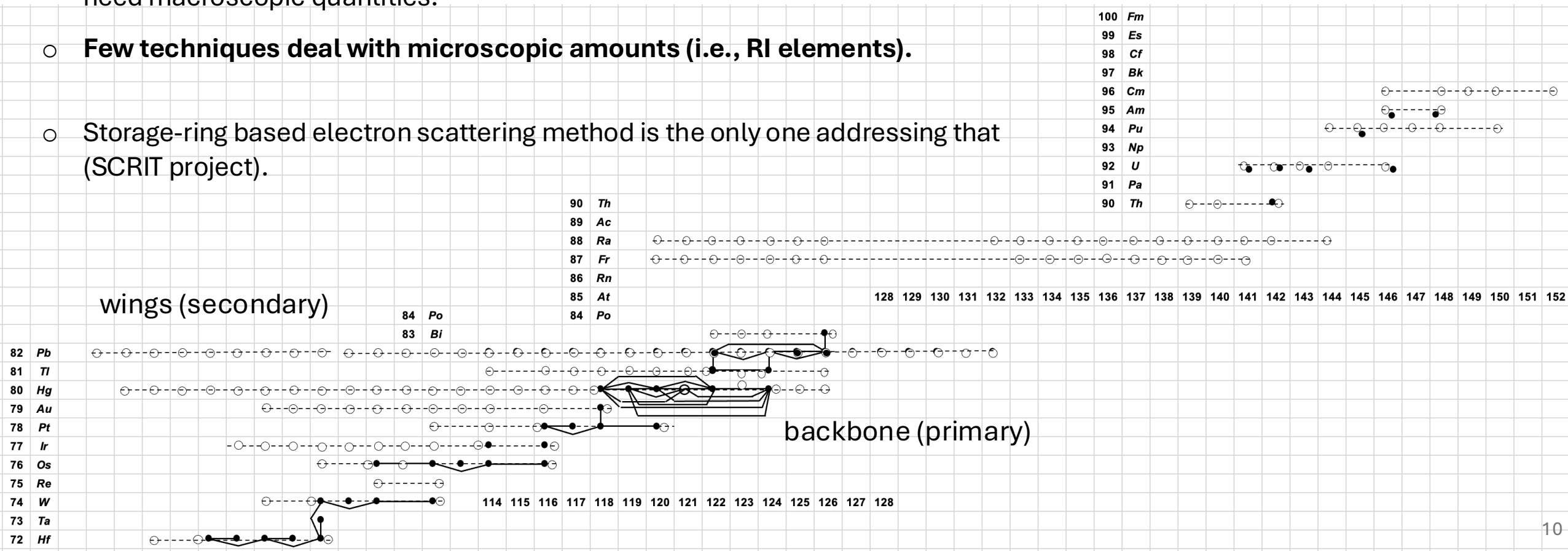
2. Spectroscopy of muonic atoms



4. Optical isotope shifts of neutral or single charged atoms

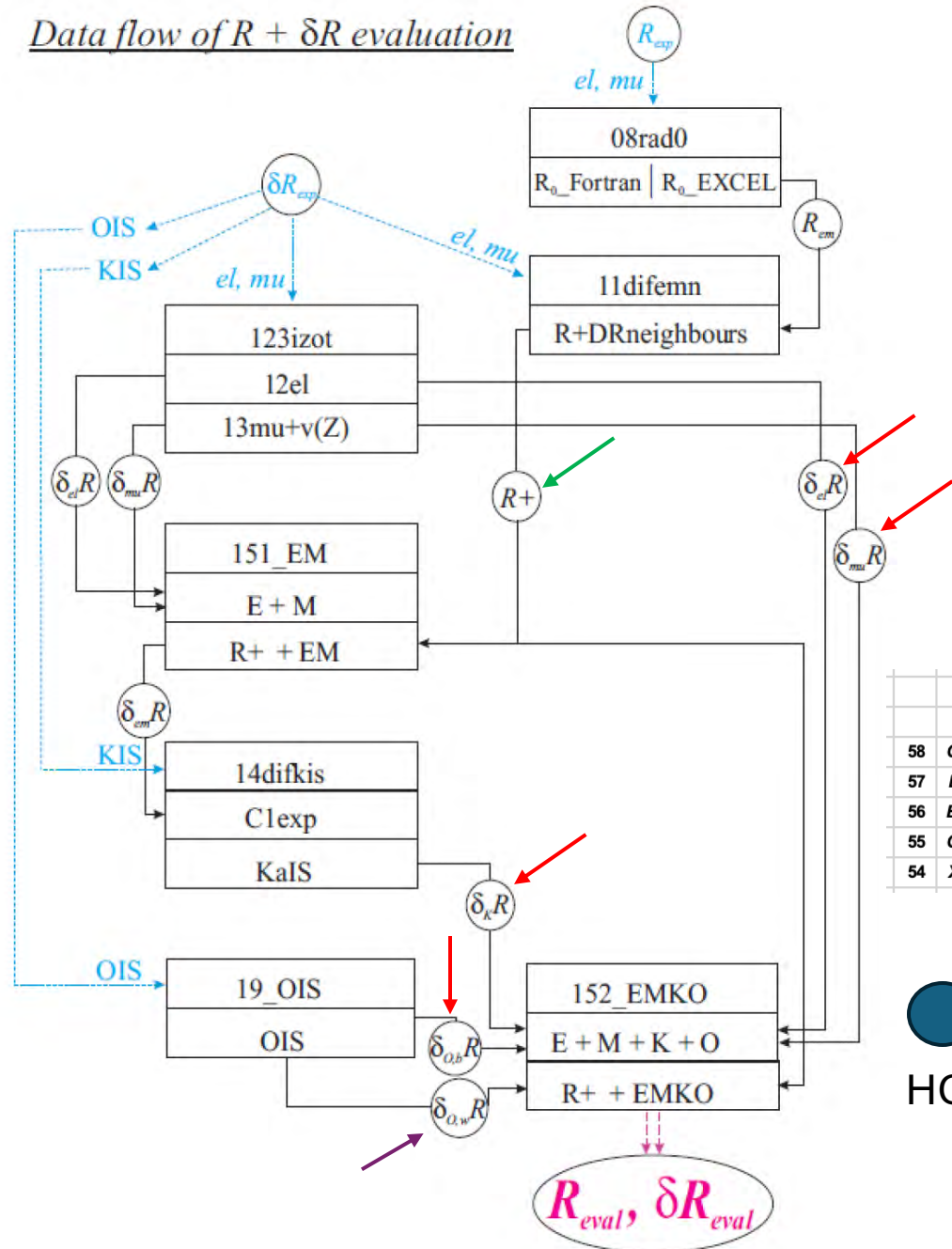
MOTIVÁCIÓ ÚJFAJTA ATOMMAG-TÖLTÉSSUGÁR MÉRÉSEKRE –NEHÉZ IONOK

- ❖ Except for a few isotopes, no **absolute** charge radius measurements for unstable isotopes exist heavier than Bi.
- The absolute charge radii of francium, radium, and radon have never been measured.
- Apparent reason: current techniques (electron scattering / muonic x-ray spectroscopy) need macroscopic quantities.
- **Few techniques deal with microscopic amounts (i.e., RI elements).**
- Storage-ring based electron scattering method is the only one addressing that (SCRIT project).



KÉNYSZERFELTÉTELEK A MAGSUGÁR FELÜLETEN

Data flow of $R + \delta R$ evaluation

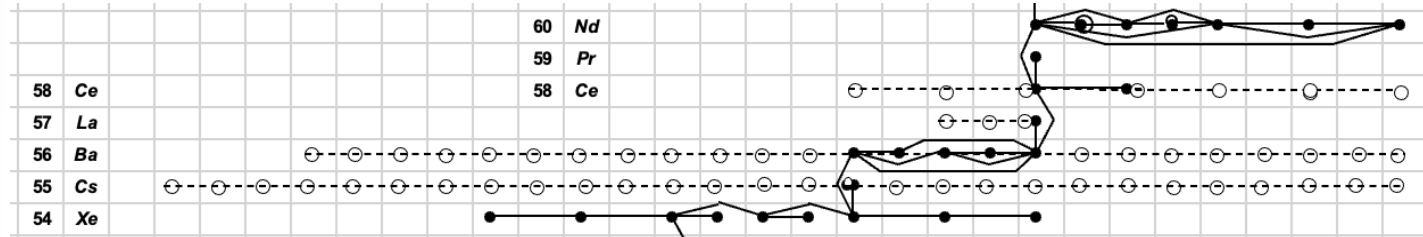


Atomic Data and Nuclear Data Tables
Volume 99, Issue 1, January 2013, Pages 69-95



Table of experimental nuclear ground state charge radii: An update

I. Angeli^a, K.P. Marinova^b



HCl

NAGYTÖLTÉSŰ IONOK

“Everyday atomic physics”

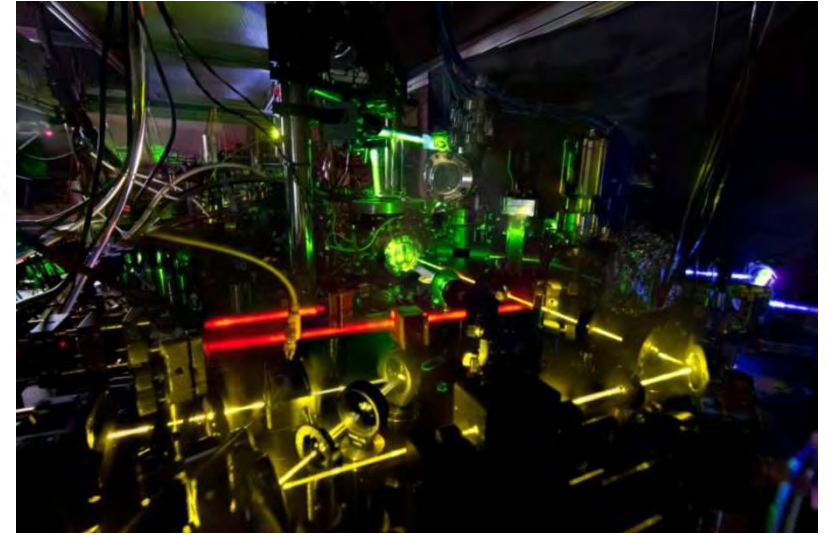
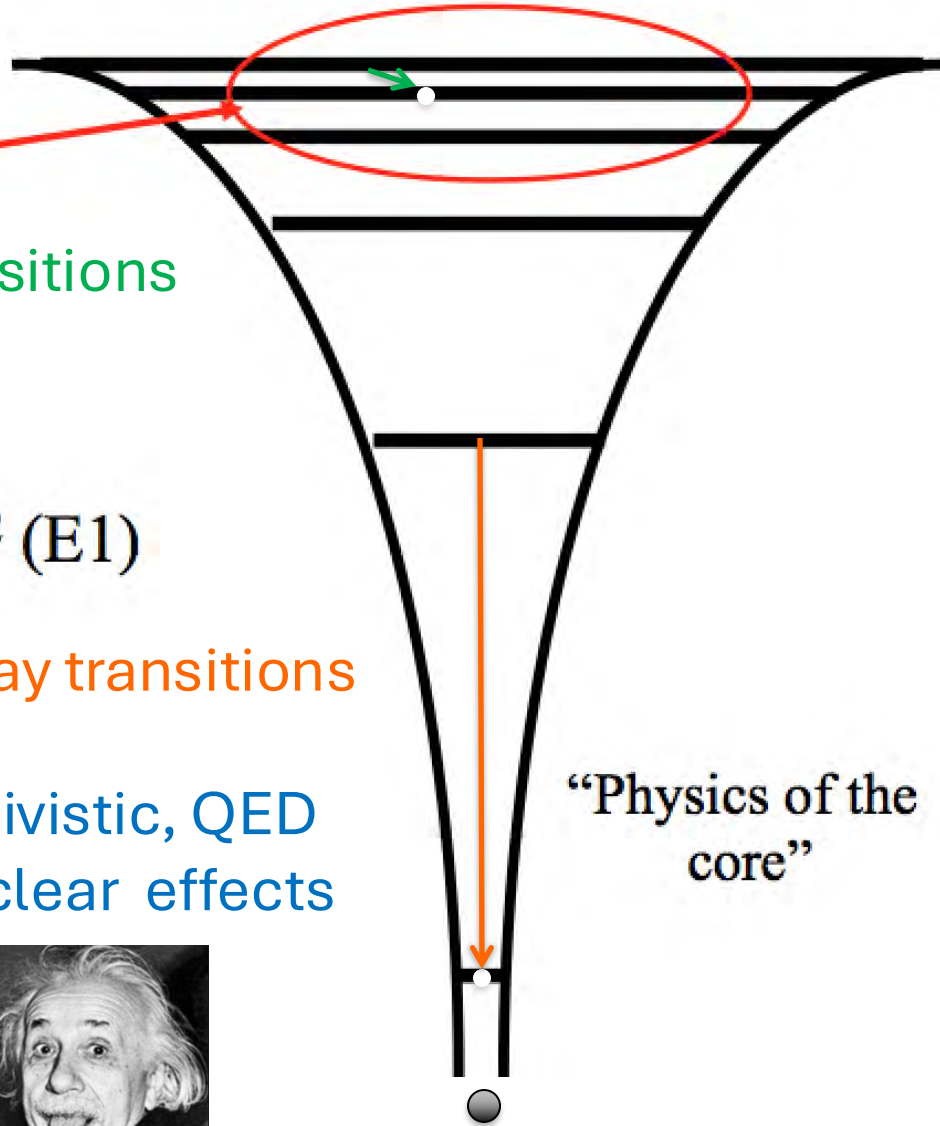
Optical transitions

Photon energy $\sim Z^2$ (E1)

X-ray transitions

Relativistic, QED
& nuclear effects

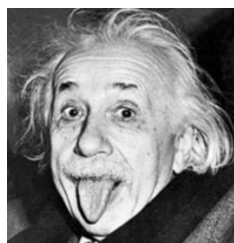
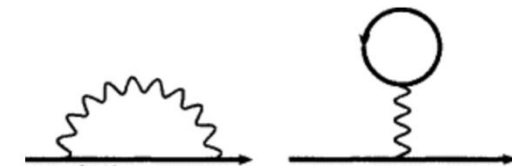
“Physics of the
core”



NIST ytterbium lattice clock



X-ray image of the solar corona



ELEKTRONNYALÁB IONCSAPDA TÖRTÉNET

Strategic Defense Initiative

Nicknamed as **Star Wars Program**, was first initiated on March 23, 1983 under President Ronald Reagan. The intent of this was to develop a sophisticated anti-ballistic missile system in order to prevent missile attacks from other countries, specifically the Soviet Union.



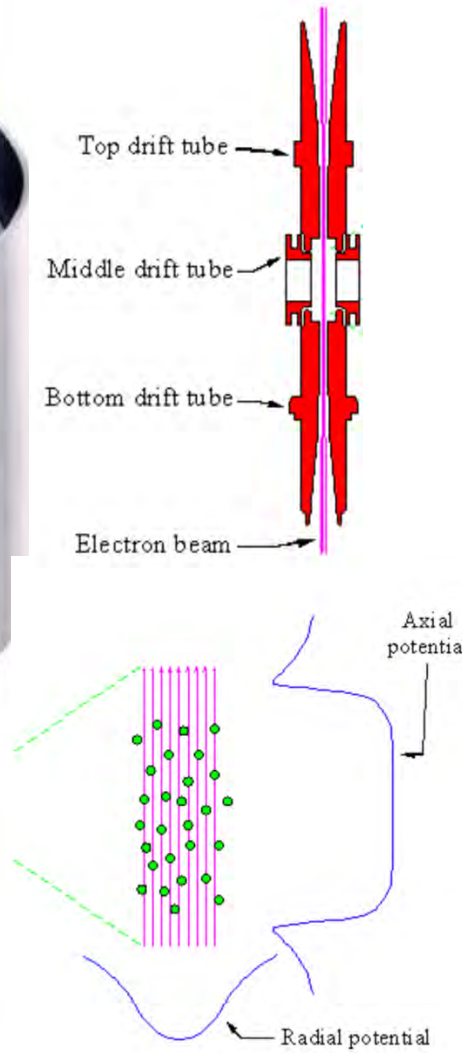
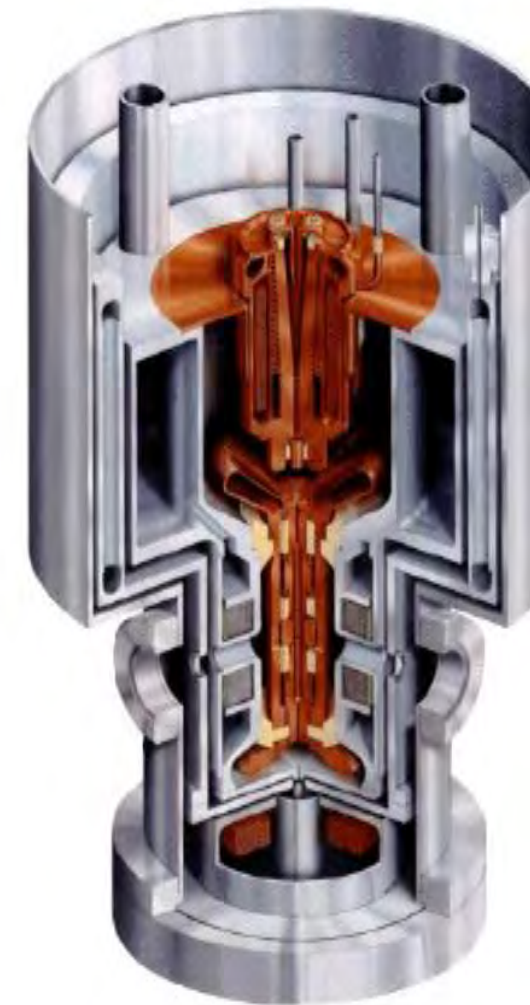
Mort Levine and Ross Marrs 1989 with the first EBIT

ELEKTRONNYALÁB IONCSAPDA TÖRTÉNET



Figure 1. The NIST EBIT, just before final assembly of the 6 major subsections (clockwise from the bottom: electron gun, drift tube assembly, collector, liquid helium insert, liquid nitrogen shield, outer vacuum can).

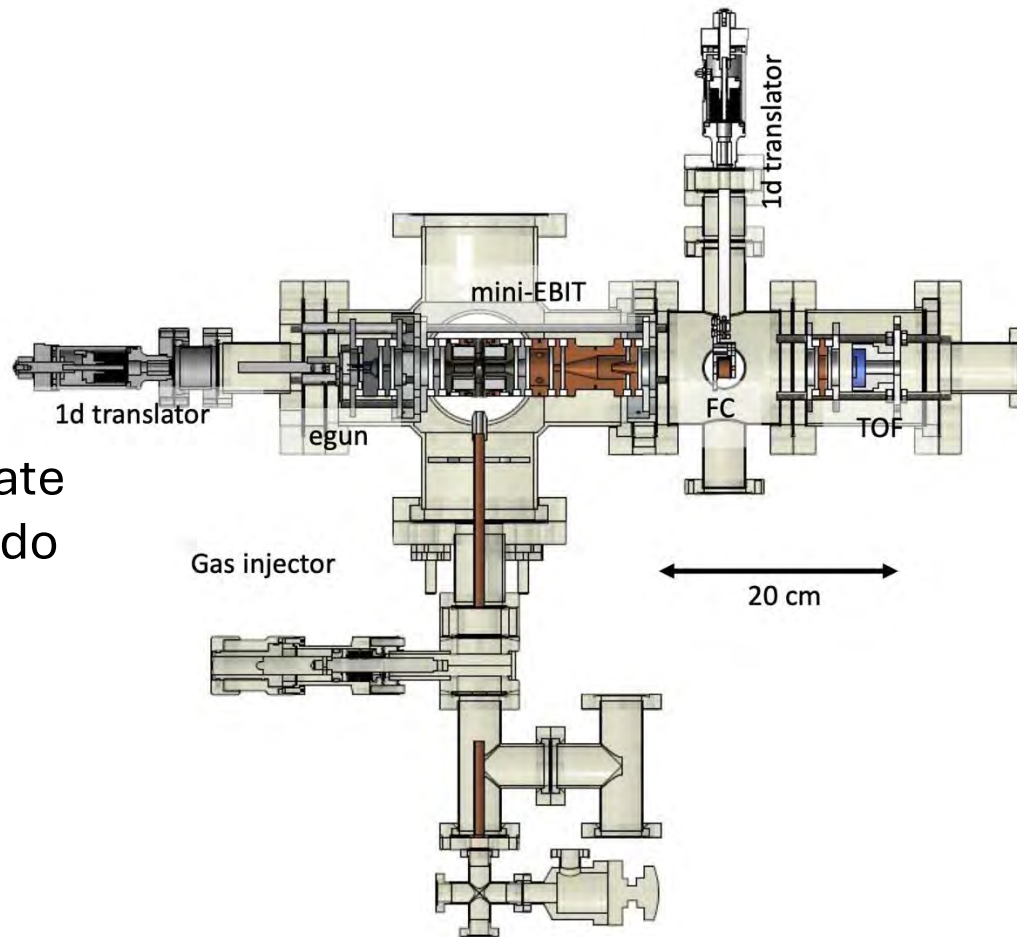
1992 NIST-NRL EBIT
(1st outside LLNL)



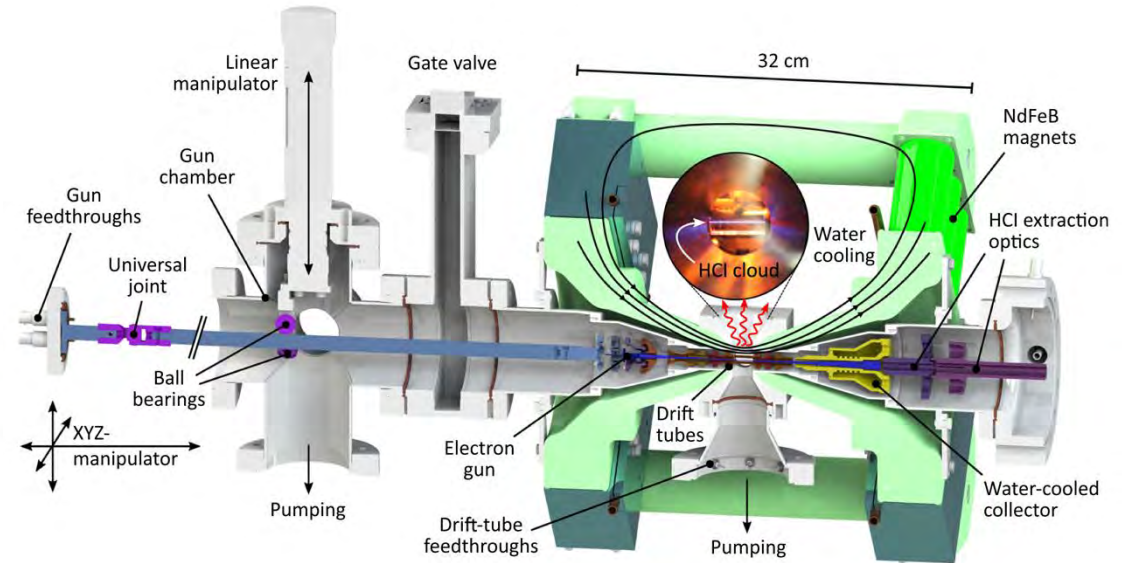
HCl spectroscopy

ÚJ KOMPAKT EBIT-EK

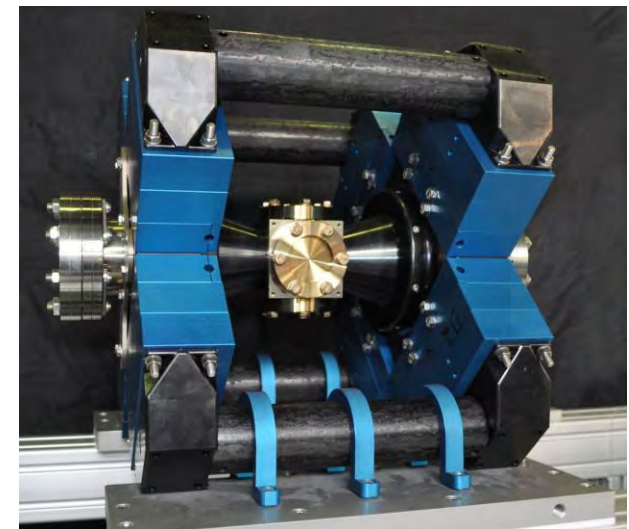
- NIST
- Heidelberg
- Tokyo
- Shanghai
- Colorado State
- Univ. Colorado
- Clemson



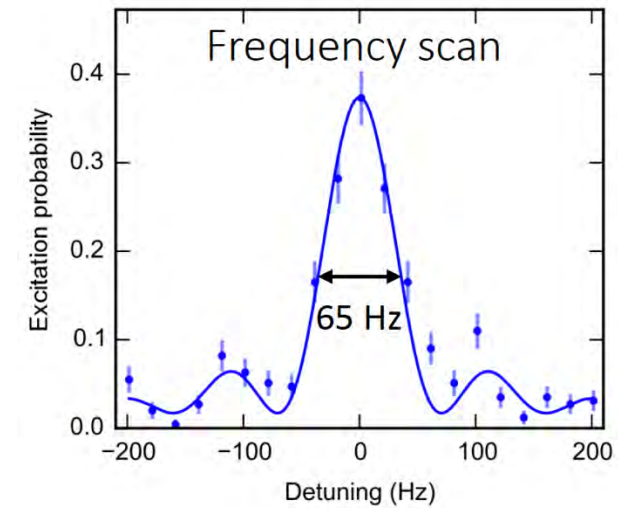
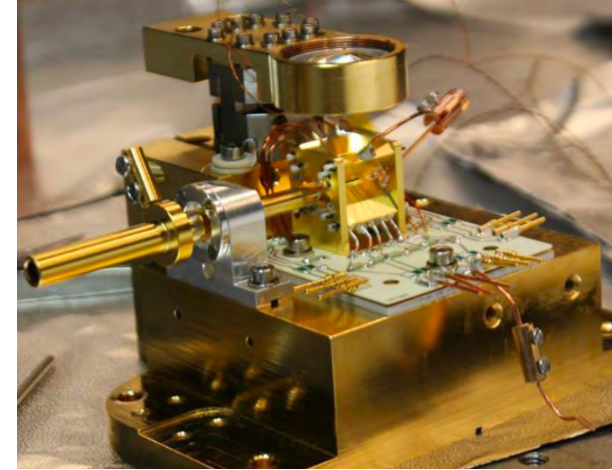
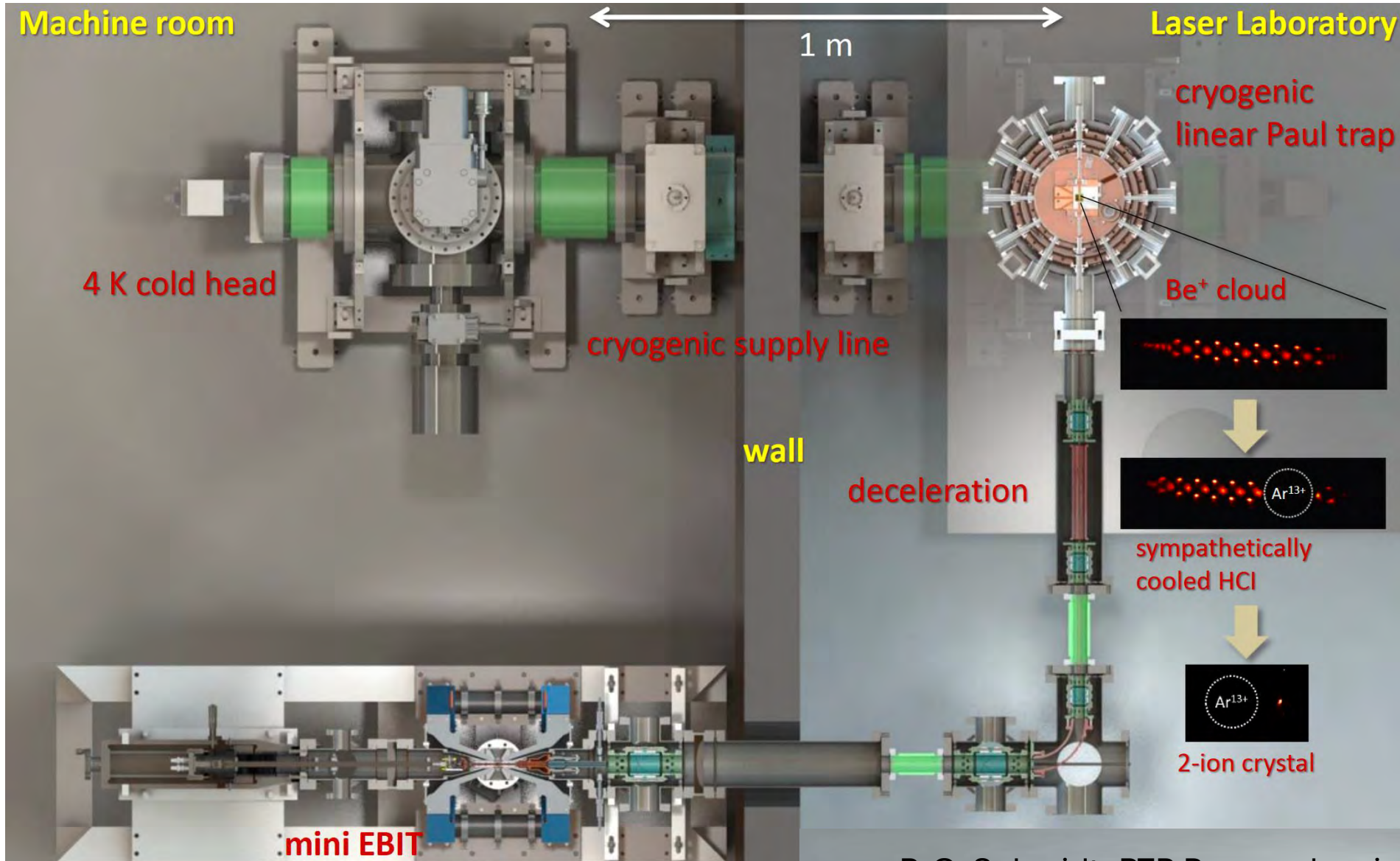
Hoogerheide and Tan, Journal of Physics:
Conference Series **583** (2015) 012044



Micke et al., Rev. Sci. Instrum. **89**, 063109 (2018)



OPTIKAI ATOMÓRA Ar^{13+} IONOKKAL (PTB ÉS MPI)

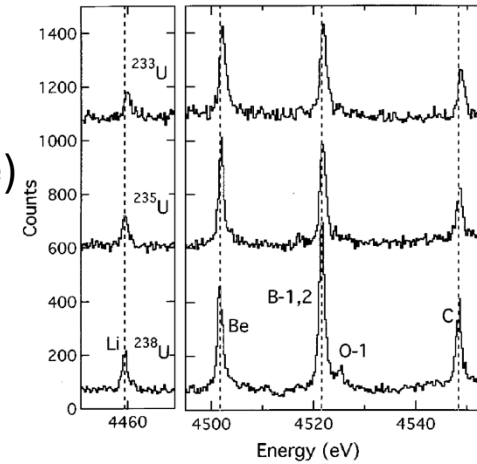


1 part in 10^{16} accuracy

NAGYTÖLTÉSŰ IONOK ÉS ATOMMAG TÖLTÉSSUGÁR

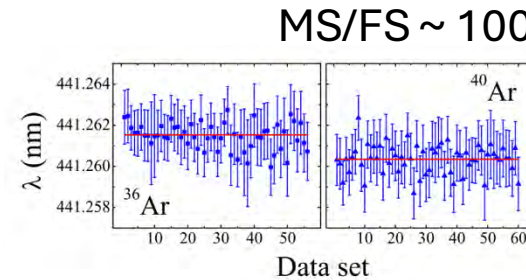
Note: mass shift scales linearly with Z – field shift scales Z^4

- Precision X-ray spectroscopy of few electron U ions (Li- through C-like)
S. R. Elliott *et al.* Phys. Rev. C **57**, 583 (1998)

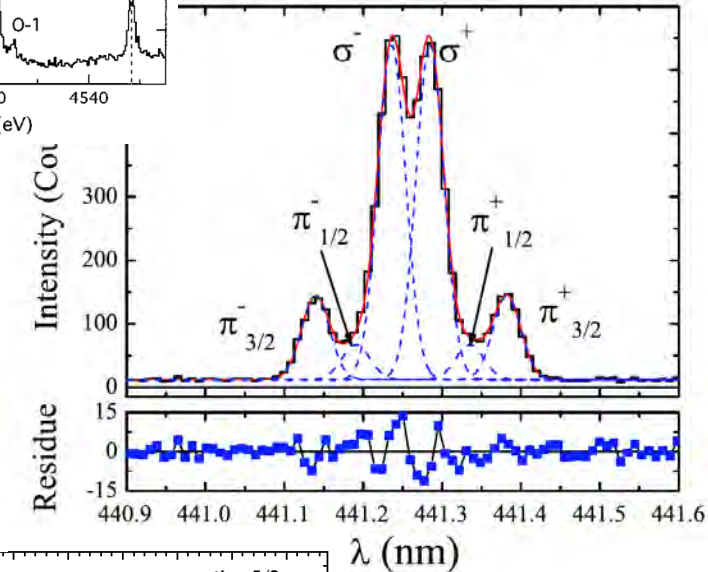


MS/FS ~ 0.03

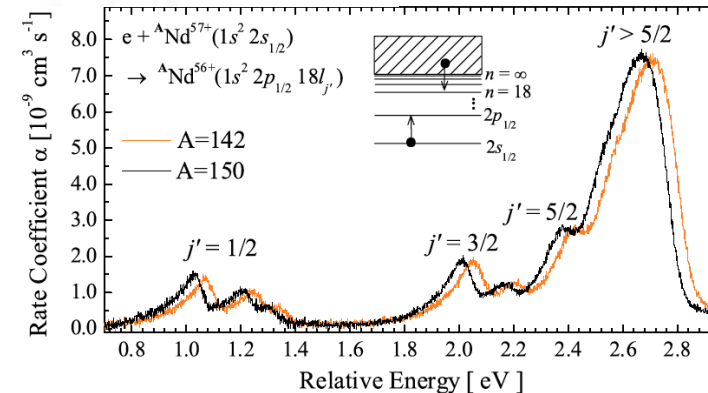
- Magnetic-dipole transitions of Be-like and B-like Ar isotopes in the visible range
R. S. Orts *et al.*, Phys. Rev. Lett. **97**, 103002 (2006)
Dissertation, Inst. fur Kernphysik Frankfurt (2005)



MS/FS ~ 100

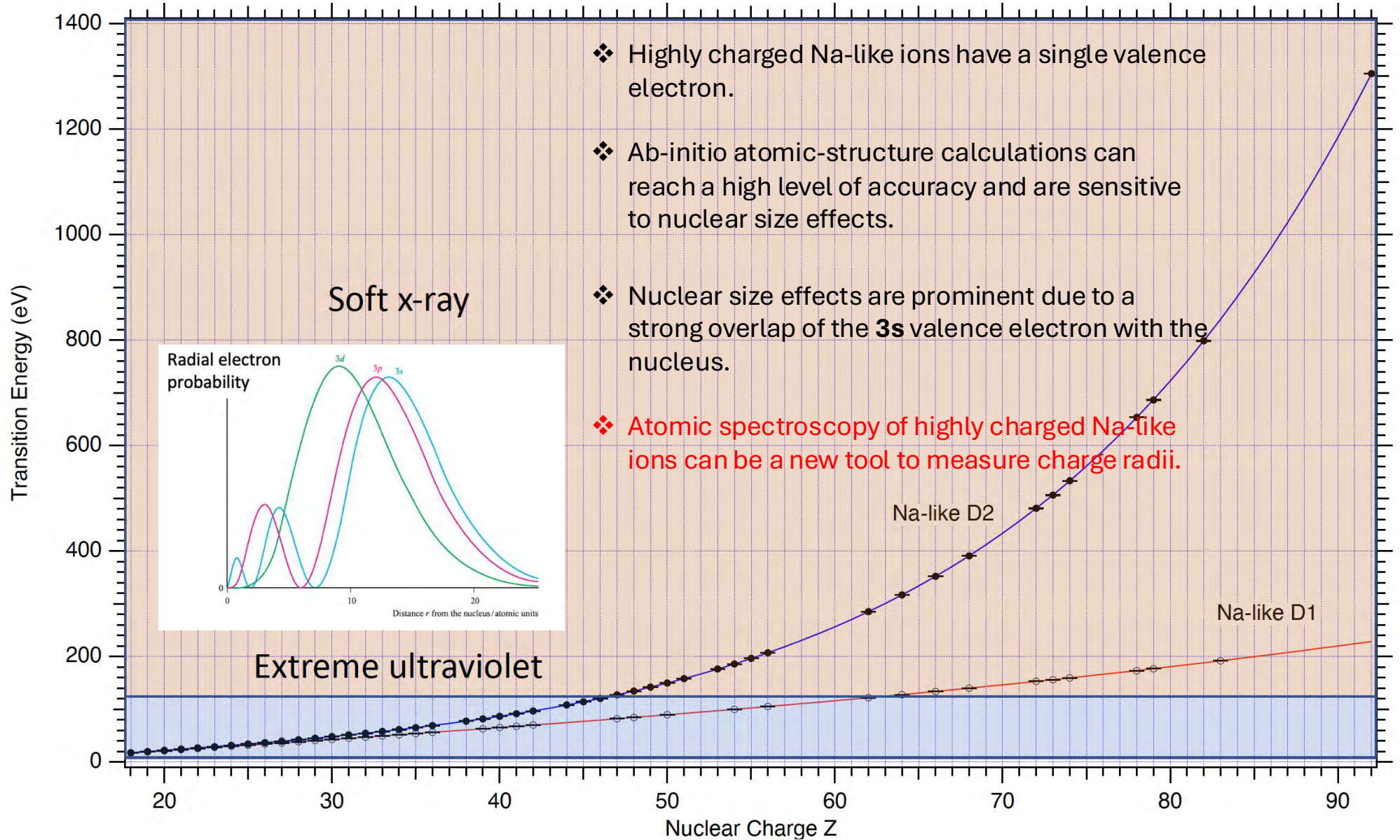
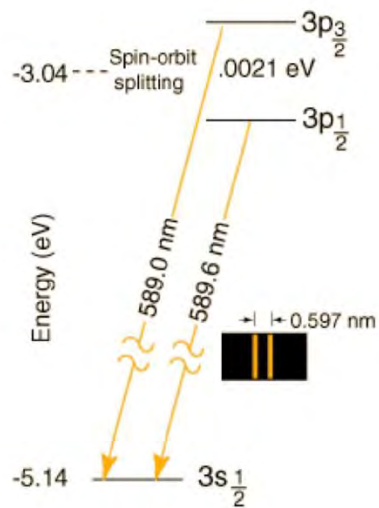
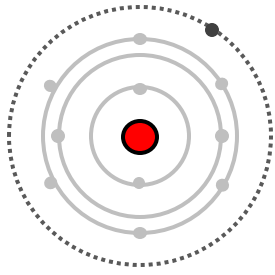


- Dielectronic recombination measurements of quasi few-electron ions (K-like Pb, Li-like Nd)
R. Schuch *et al.*, Phys. Rev. Lett. **95**, 183003 (2005)
C. Brandau *et al.*, Phys. Rev. Lett. **100**, 073201 (2008)



MS/FS ~ 0.5

NÁTRIUMSZERŰ IONOK

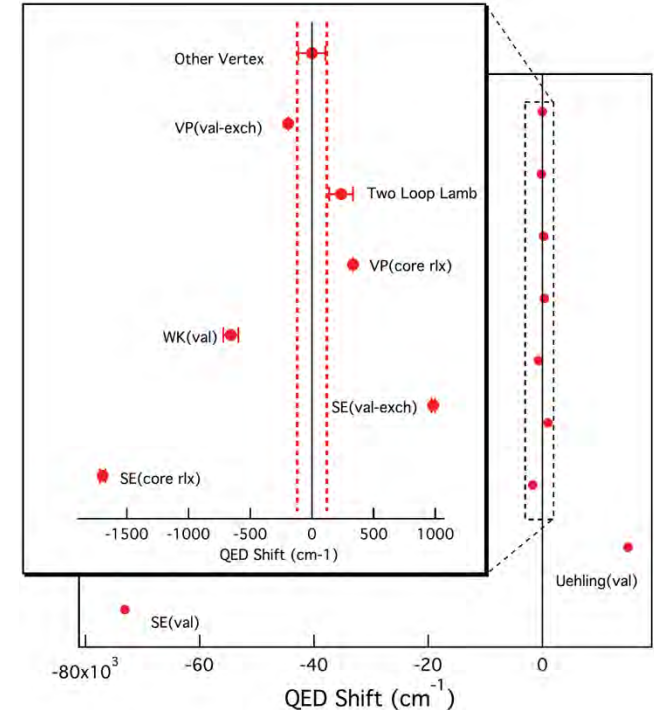
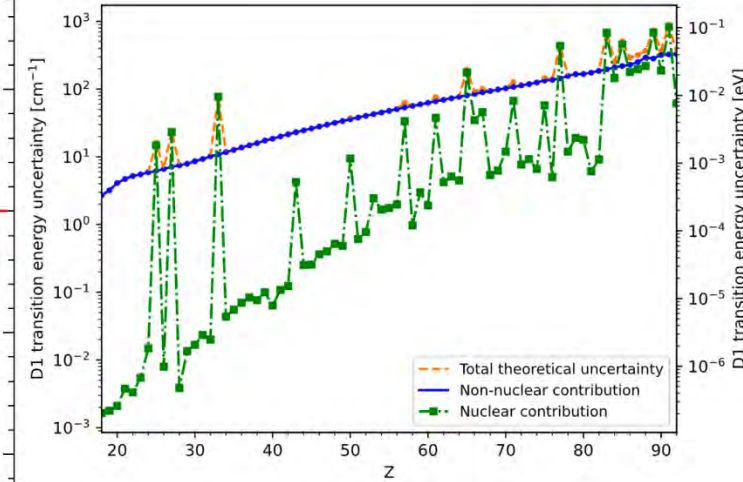
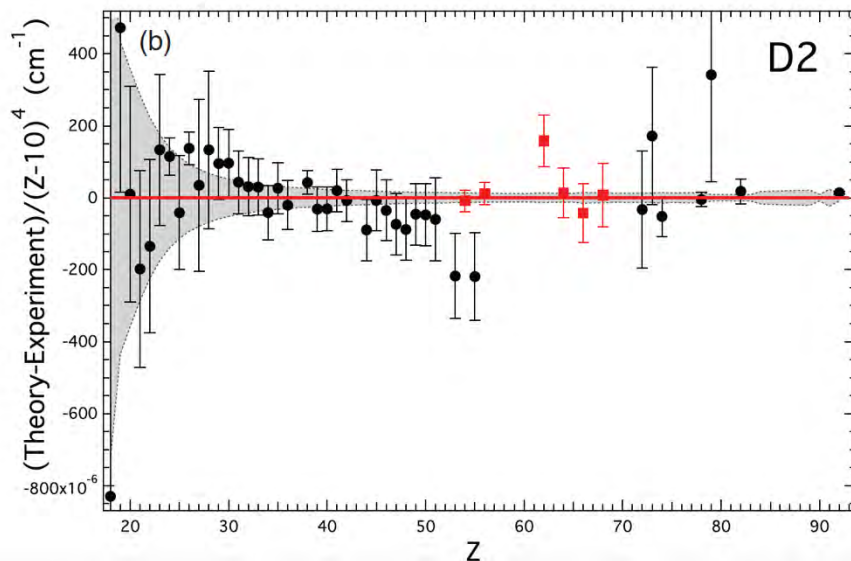
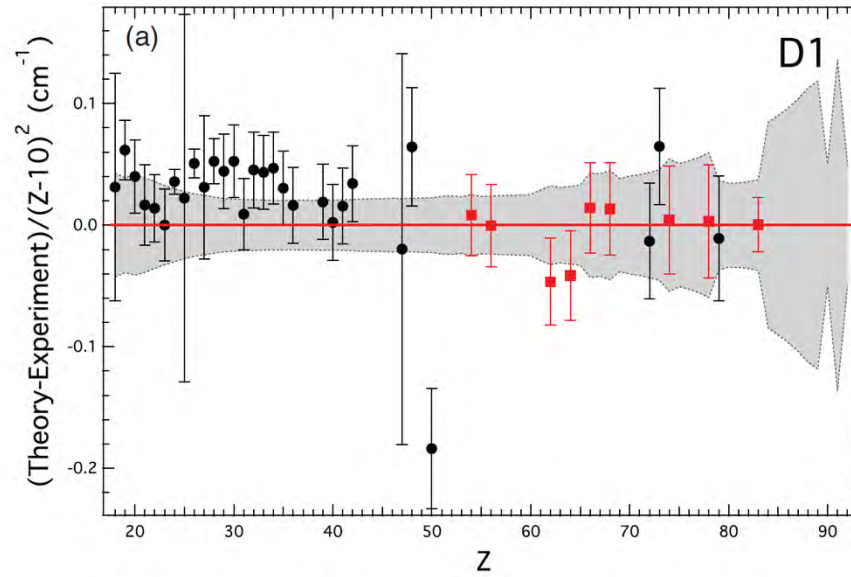


- ❖ Highly charged Na-like ions have a single valence electron.
- ❖ Ab-initio atomic-structure calculations can reach a high level of accuracy and are sensitive to nuclear size effects.
- ❖ Nuclear size effects are prominent due to a strong overlap of the **3s** valence electron with the nucleus.
- ❖ Atomic spectroscopy of highly charged Na-like ions can be a new tool to measure charge radii.

STATE-OF-THE-ART AB INITIO ELMÉLETEK (RMBPT, MCDHF, S-MATRIX)

TABLE III. Contributions (cm^{-1}) to the total calculated wave numbers σ and their estimated uncertainties for Bi ($Z = 83$). Values between the dotted lines are from the QED terms.

	$\sigma(D_1)$	Unc.	$\sigma(D_2)$	Unc.
Dirac Hartree Fock	1 559 528	37	6 836 929	41
B(1)	52 830	0	-1481	0
B(rpa)	-1238	0	-299	0
BB(rpa)	-127	0	15	0
Ret(1)	499	0	-8402	0
Ret(rpa)	53	0	-70	0
Other retardation	0	107	0	209
CC(2)	-2616	2	-354	1
BC(2)	-544	1	-265	0
CCC(3)	16	0	-7	0
Nuclear recoil	-68	25	-76	28
.....				
SE(val)	-73 091	3	-71 432	3
Uehling (val)	15009	0	17 318	0
WK (val)	-657	62	-781	50
SE (val-exch)	983	14	1029	14
VP (val-exch)	-192	0	-200	0
SE (core rx)	-1697	23	-814	11
VP (core rx)	334	0	186	0
Other vertex	0	110	0	73
Two-loop Lamb (val)	238	96	222	90
.....				
Total	1 549 261	199	6 771 519	249



NÁTRIUMSZERŰ IONOK – KÍSÉRLETI MEGFONTOLÁSOK

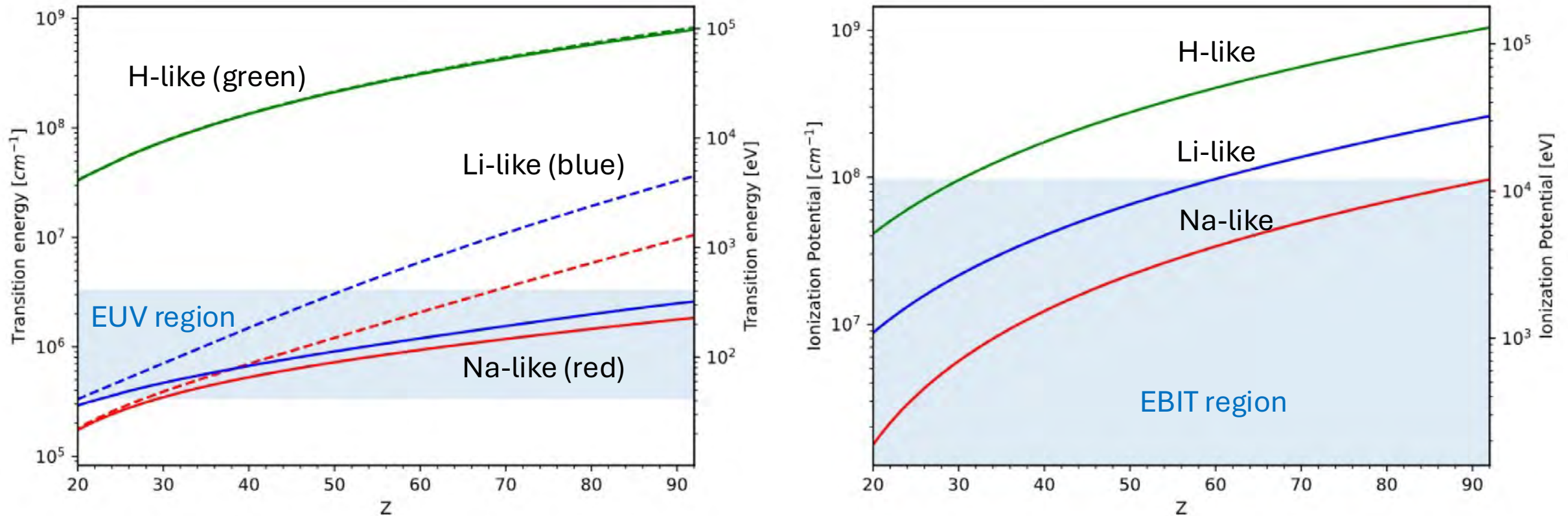
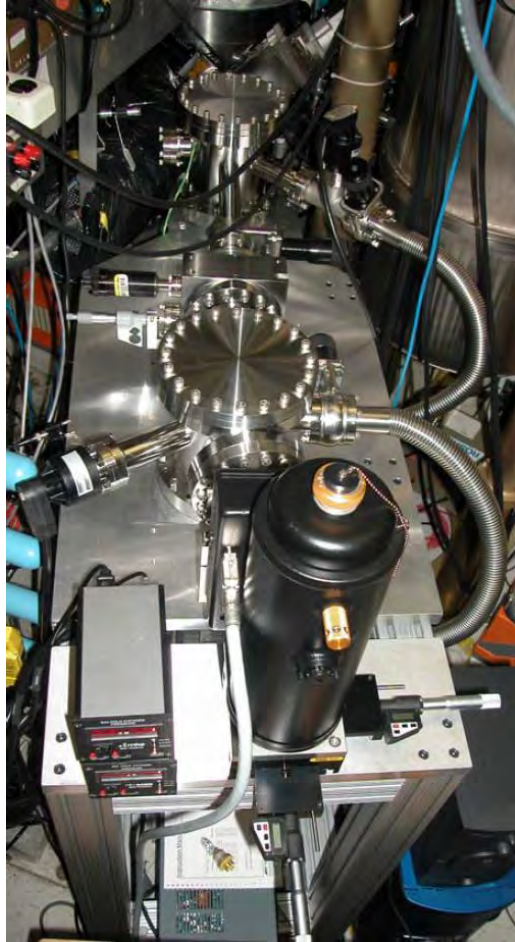


Figure 1: (Left) Plot of transition energies from $Z = 20$ to $Z = 92$, with Na-like D1 $3s^2S_{1/2} \rightarrow 3p^2P_{1/2}$ [23] (red solid), Na-like D2 $3s^2S_{1/2} \rightarrow 3p^2P_{3/2}$ [23] (red dashed), Li-like $1s^22s^2S_{1/2} \rightarrow 1s^22p^2P_{1/2}$ [24] (blue solid), Li-like $1s^22s^2S_{1/2} \rightarrow 1s^22p^2P_{3/2}$ [24] (blue dashed), H-like $1s^2S_{1/2} \rightarrow 2p^2P_{1/2}$ [25] (green solid), and H-like $1s^2S_{1/2} \rightarrow 2p^2P_{3/2}$ [25] (green dashed). The shaded blue region indicates EUV range (3 to 30 nm). (Right) Plot of ionization potential necessary to create Na-like (red), Li-like (blue) and H-like (green) ions. The shaded blue region indicates the typical range of optimum electron beam energies used to generate highly charged ions [26]). Hosier et al., Journal of Physics B **57**, (2024) 195001

NÁTRIUMSZERŰ IONOK MÉRÉSI MÓDSZEREI

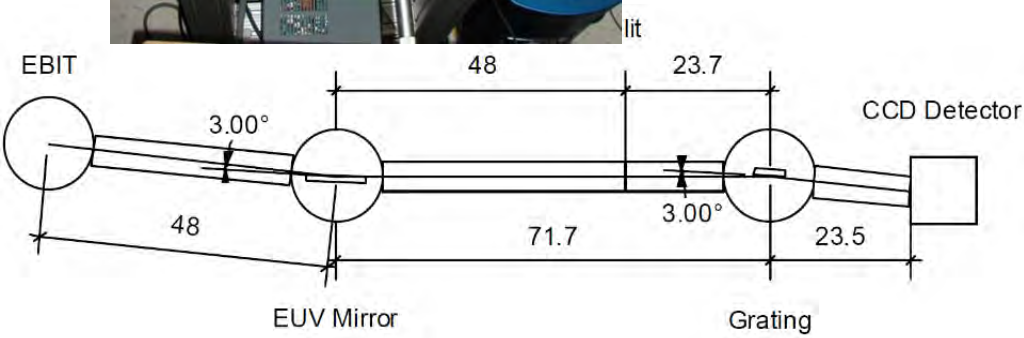
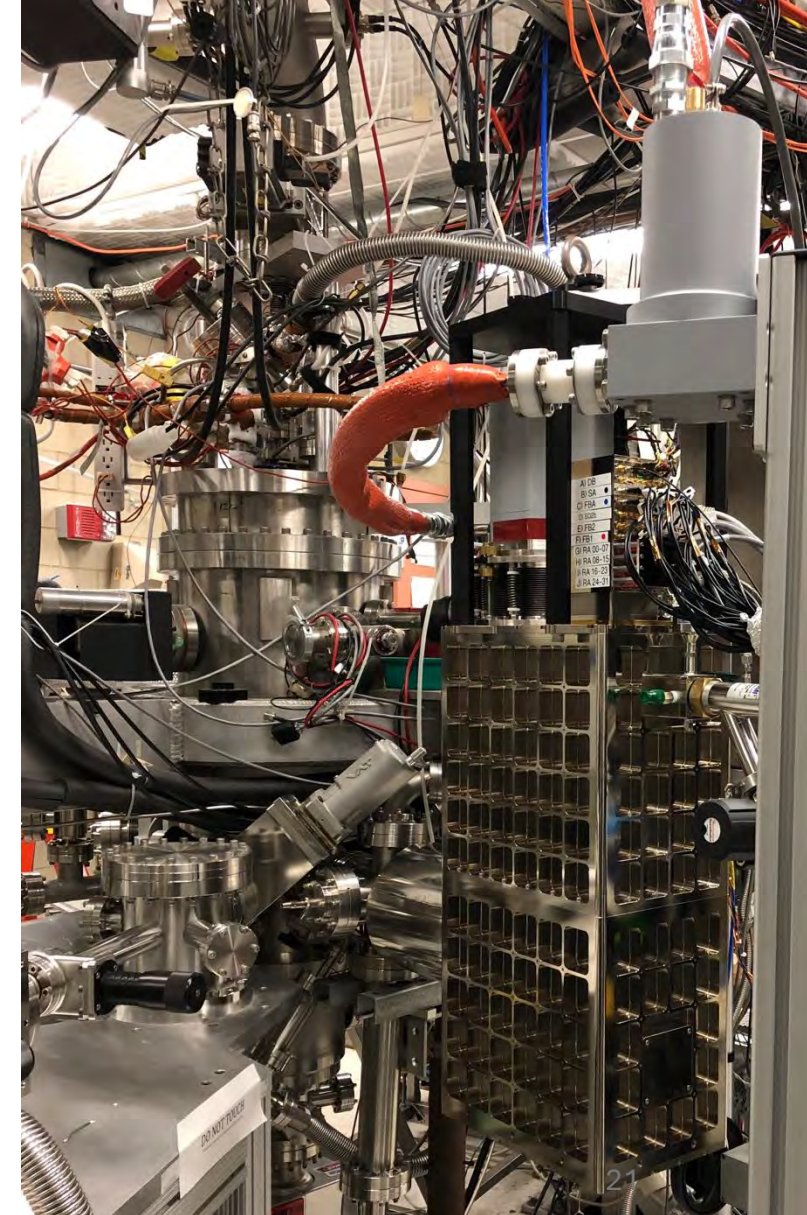
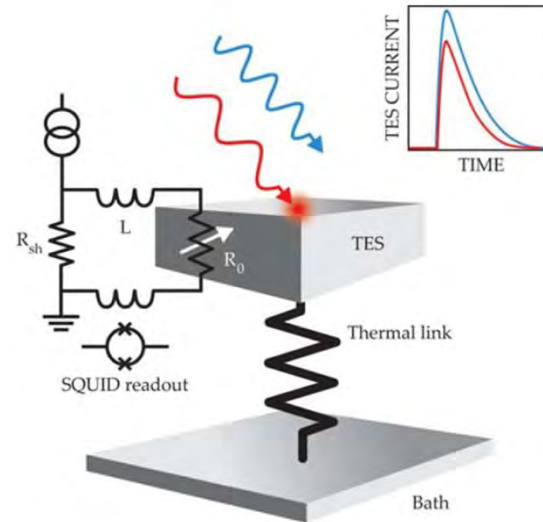


NIST EBIT

X-ray



EUV



KÉT NÁTRIUMSZERŰ IZOTÓP D VONALÁNAK TÁVOLSÁGA

Silwal R et al., Phys. Rev. A **98** (2018) 052502; Silwal R et al., Phys. Rev. A **101** (2020) 062512

$$\delta E_k^{A,A'}(Exp.) = E_k^A - E_k^{A'} = \text{Mass shift} + \text{Field shift}$$


$$\begin{aligned} \delta E_k^{A,A'} &= \delta E_{k,MS}^{A,A'} + \delta E_{k,FS}^{A,A'} \\ &= (\text{NMS} + \text{SMS}) \frac{(M' - M)}{MM'} + F \lambda^{A,A'} \end{aligned}$$

átlag-sugár jelölésére bevezettük az $\langle r^2 \rangle \equiv \int \rho(r) r^2 dv$ szimbólumot szimbólumot (ennek négyzetgyöke a *root-mean square: rms*).

$$\delta E_{FS}^{A,A'} = F_0 \delta \langle r^2 \rangle^{A,A'} + F_2 \delta \langle r^4 \rangle^{A,A'} + F_6 \delta \langle r^6 \rangle^{A,A'} + F_8 \delta \langle r^8 \rangle^{A,A'} + \dots$$

$$= \left[F_0 + F_2 \frac{\delta \langle r^4 \rangle^{A,A'}}{\delta \langle r^2 \rangle^{A,A'}} + F_6 \frac{\delta \langle r^6 \rangle^{A,A'}}{\delta \langle r^2 \rangle^{A,A'}} + F_8 \frac{\delta \langle r^8 \rangle^{A,A'}}{\delta \langle r^2 \rangle^{A,A'}} + \dots \right] \delta \langle r^2 \rangle^{A,A'}$$

$$= F \delta \langle r^2 \rangle^{A,A'}$$

KÍSÉRLETI  MAGFIZIKA
(BSc)

Angeli István

$$\delta \langle r^2 \rangle^{A,A'} = \frac{\delta E_k^{A,A'}(Exp.) - \delta E_{k,MS}^{A,A'}}{F}$$

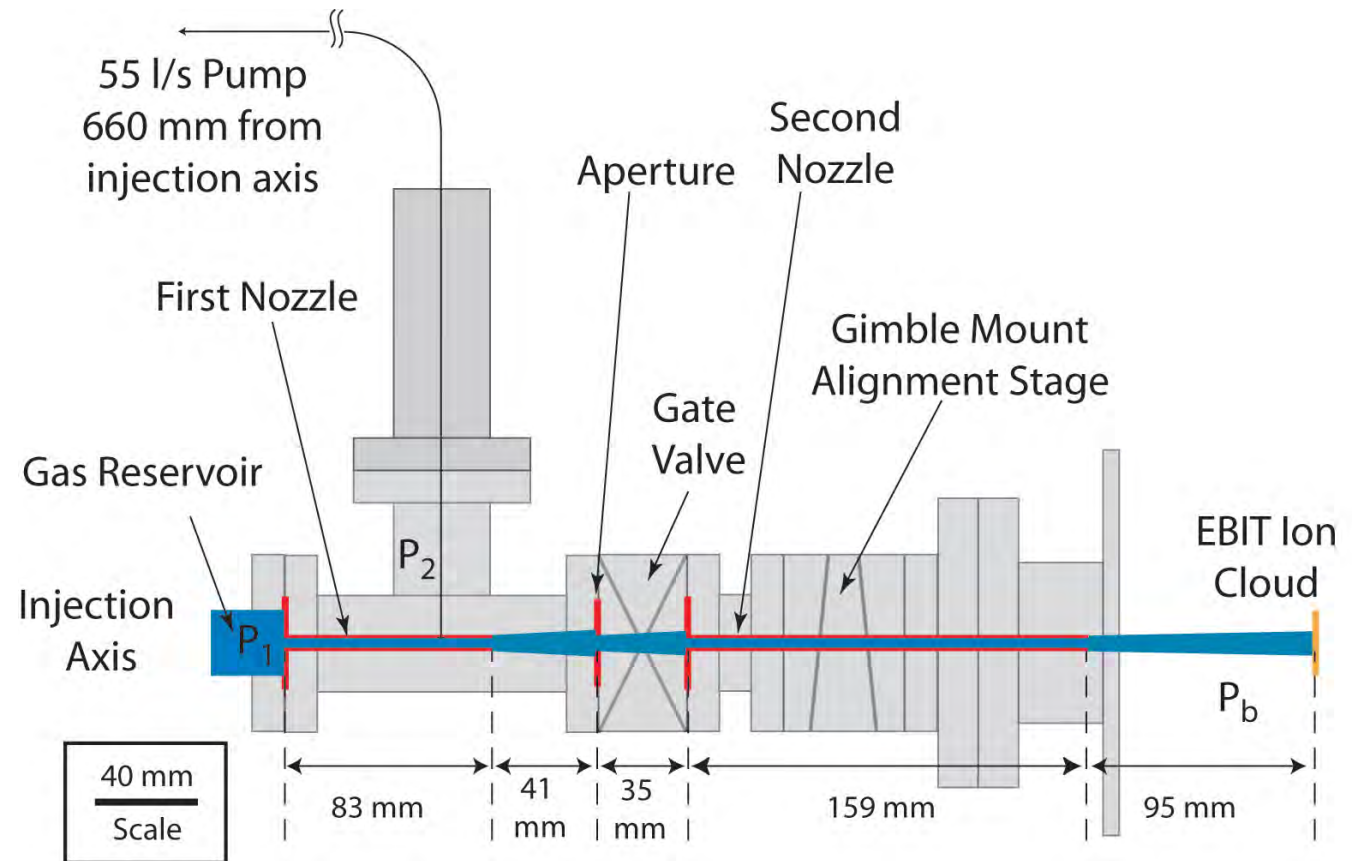
RMBPT or MCDHF calculates these accurately for Na-like ions (with uncertainties)

(Steven Blundell RMBPT, Dipti GRASP2K)

IZOTÓP TISZTA Xe¹³⁶ ÉS Xe¹²⁴ SEMLEGES ATOMOK EBIT-BE JUTTATÁSA



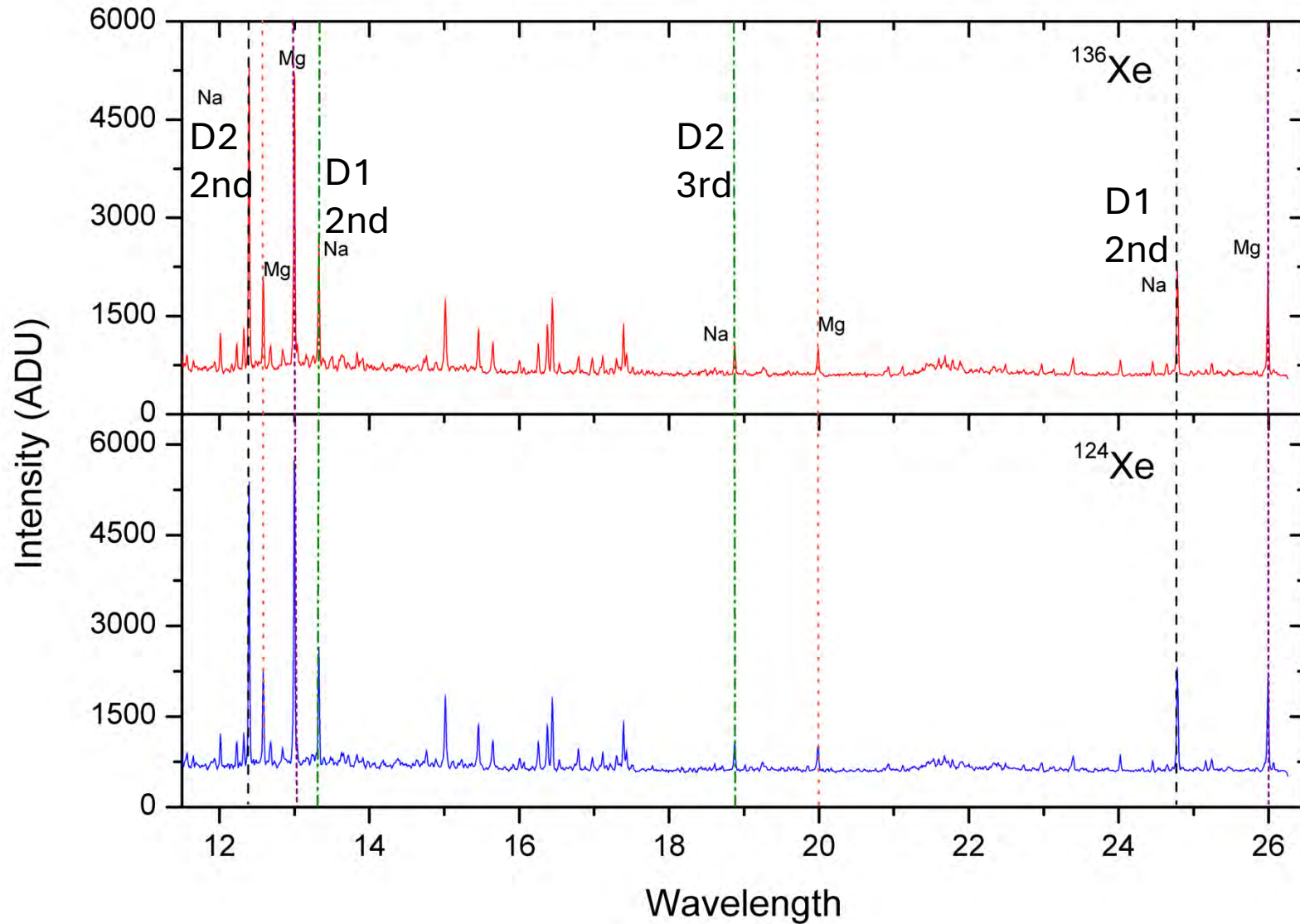
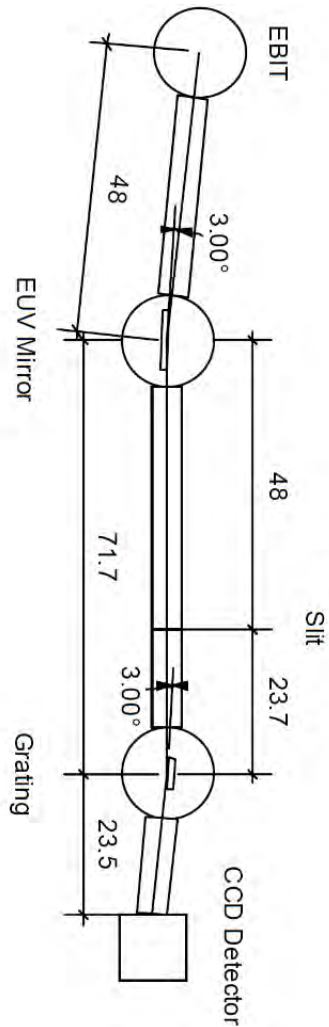
- both have zero magnetic moment
- no hyperfine effect
- discrepancy exists between muonic and optical measurements



ELSŐ KÍSÉRLET: ^{136}Xe and ^{124}Xe EUV SPEKTROSKÓPIA

6 keV beam energy, 150 mA beam current

alternating injection in every hour, 5 minutes spectra, for 5 days

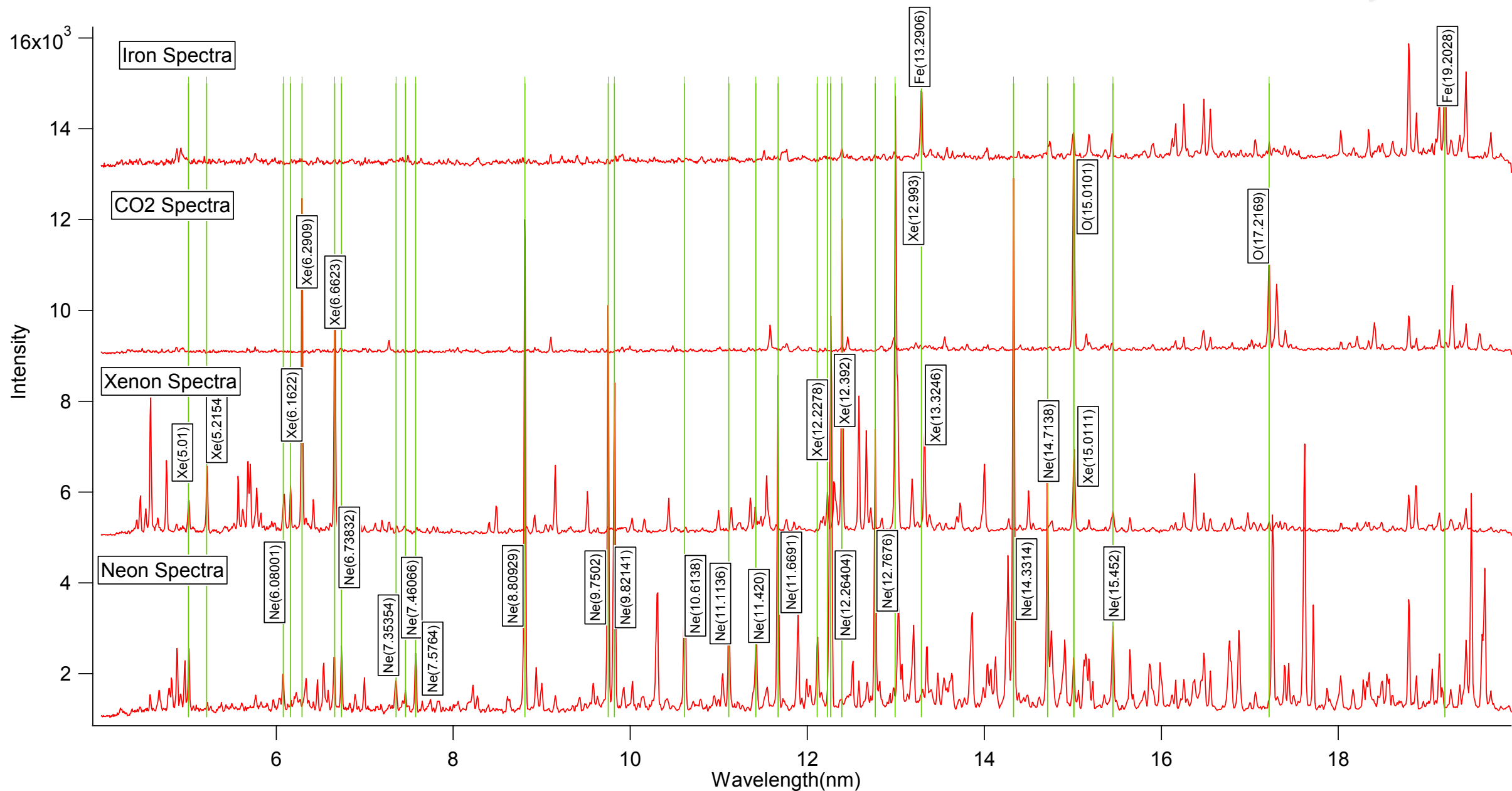


PONTOS EUV KALIBRÁCIÓ A NIST-BEN

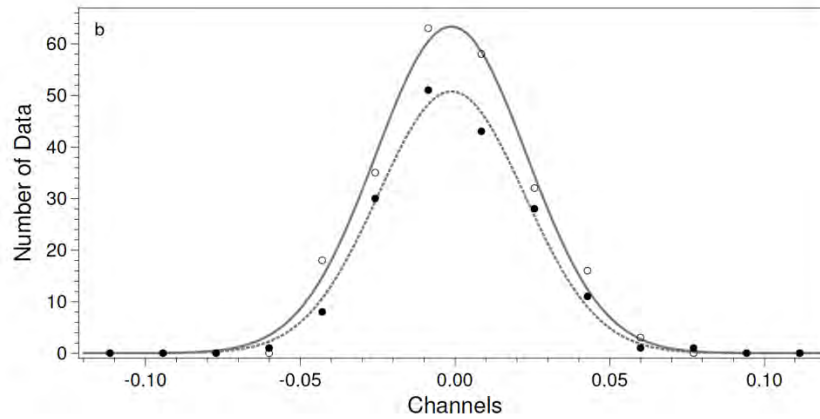
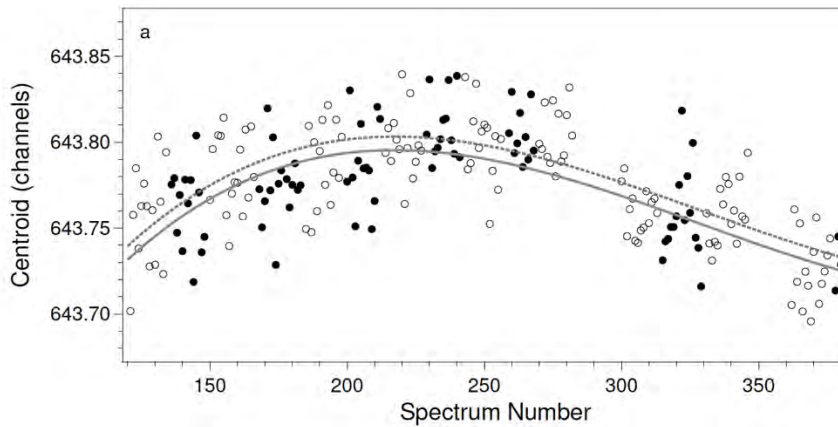


DATA
LINES LEVELS

NIST
National Institute of
Standards and Technology
Physical Meas. Laboratory



IZOTÓP ELTOLÓDÁS



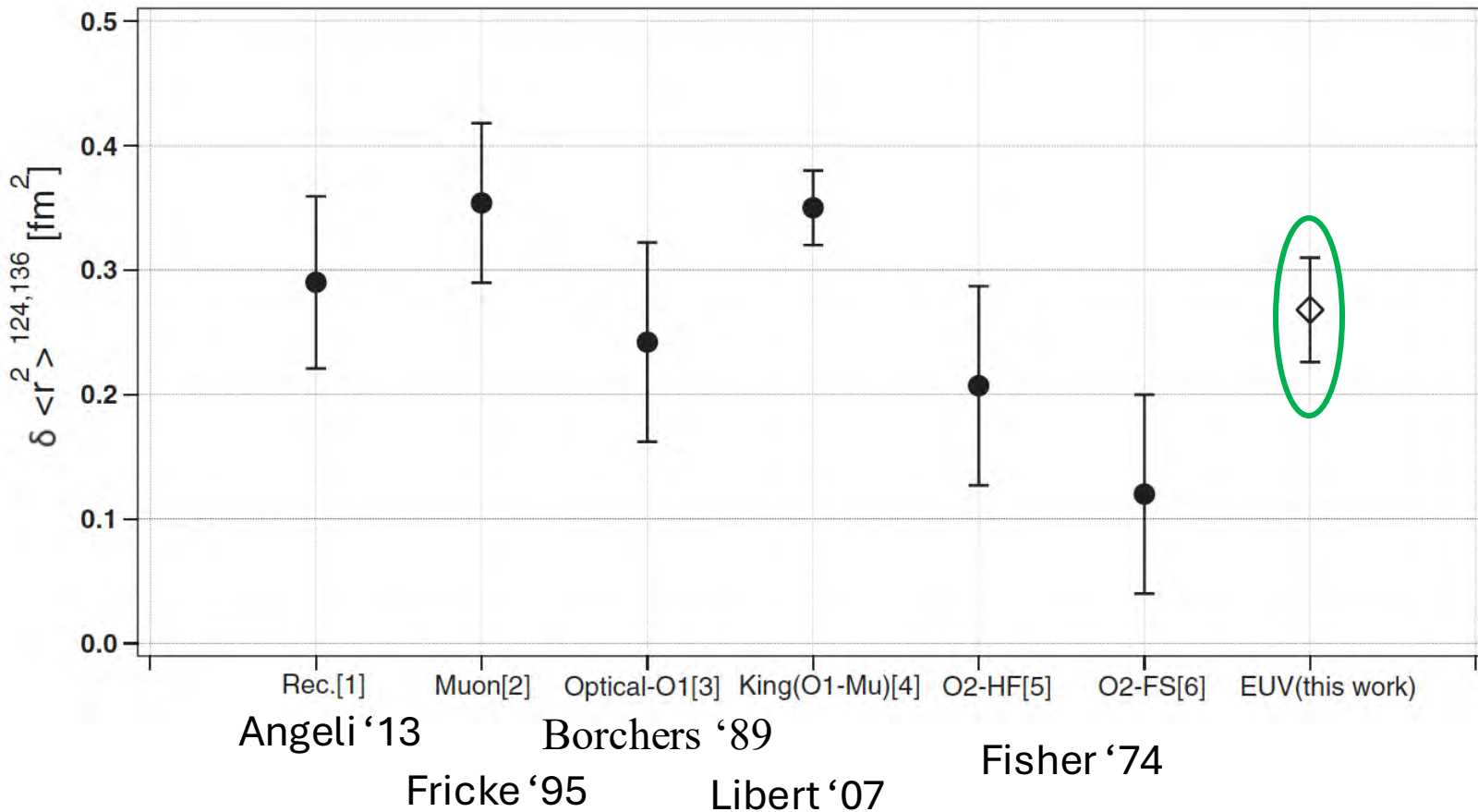
The systematic drift was fitted with an overall function of piece-wise 3rd order polynomials that included a shift between the isotopes (one hundredth of a pixel)

TABLE I. Measured and calculated wavelength values of the isotope shift along with their uncertainties (in units of fm) for the Na-like $D1$ transition $3s\ ^2S_{1/2} - 3p\ ^2P_{1/2}$ for the isotope pair $^{136}\text{Xe}-^{124}\text{Xe}$. The field shift was calculated using the evaluated value of 0.290 fm^2 for $\delta\langle r^2\rangle^{136,124}$ by [20].

Coefficients	Theory					Experiment	
	RMBPT		GRASP2K		CIDF [29]	$\delta\lambda$	$\Delta\delta\lambda$
	$\delta\lambda$	$\Delta\delta\lambda$	$\delta\lambda$	$\Delta\delta\lambda$	$\delta\lambda$	$\delta\lambda$	$\Delta\delta\lambda$
NMS	-4.8	0.2	-4.8	0.2	-4.8		
SMS	-62.2	3.4	-62.3	3.4	-62.7		
Total MS	-67.0	3.4	-67.1	3.4	-67.5		
FS	143.0	2.8	142.0	2.8	143.0		
Total	76.1	4.4	75.3	4.4	75.8	65.5	20.6 fm

MAGSUGÁR KÜLÖNBSÉG: $^{136}\text{Xe} - ^{124}\text{Xe}$

Silwal R et al., Phys. Rev. A **98** (2018) 052502; Silwal R et al., Phys. Rev. A **101** (2020) 062512



Rec. - Angeli and Marinova

Muon - Muonic atoms

O1 - Optical shift

Exp. Unc.: **0.005 fm²**

Theor. Unc.: **0.080 fm²**

King - King plot

O2-HF - OS + Hartree-Fock

O2-FS - OS+ Fermi-Segre

EUV- Present

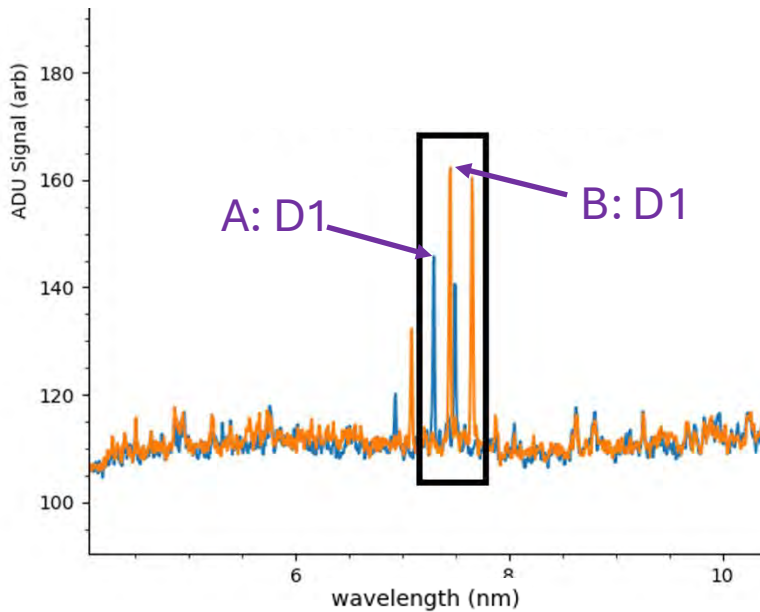
Total Unc.: **0.042 fm²**

Theor. Unc.: **0.005 fm²**

$$\delta \langle r^2 \rangle^{136,124} = 0.269(42) \text{ fm}^2$$

ABSZOLÚT MAG RMS TÖLTÉSSUGÁR D VONAL TÁVOLSÁGOKBÓL

Hosier et al., Atoms **11** (2023) 48; Hosier et al., Journal Physics B, **57** (2024) 195001;
 Hosier et al., Physical Review Research, (2025) **In print**



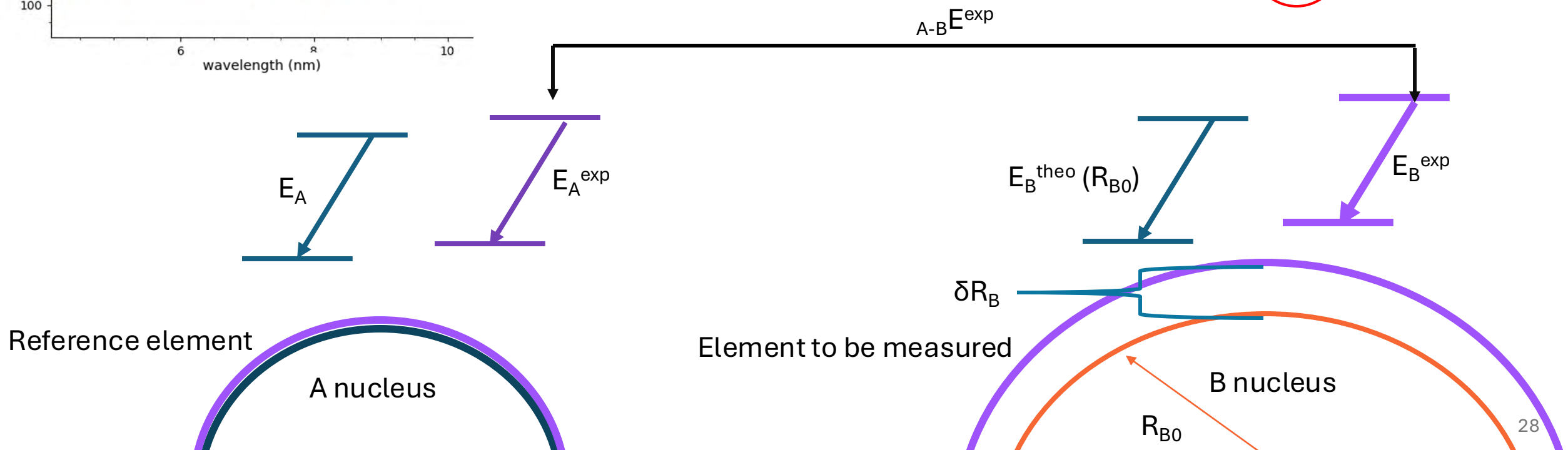
$$\delta E_{AB} \equiv E_{A-B}^{\text{exp}} - E_{A-B}^{\text{th}}$$

theoretical difference
 has reduced uncertainty
 (factor of 10!)

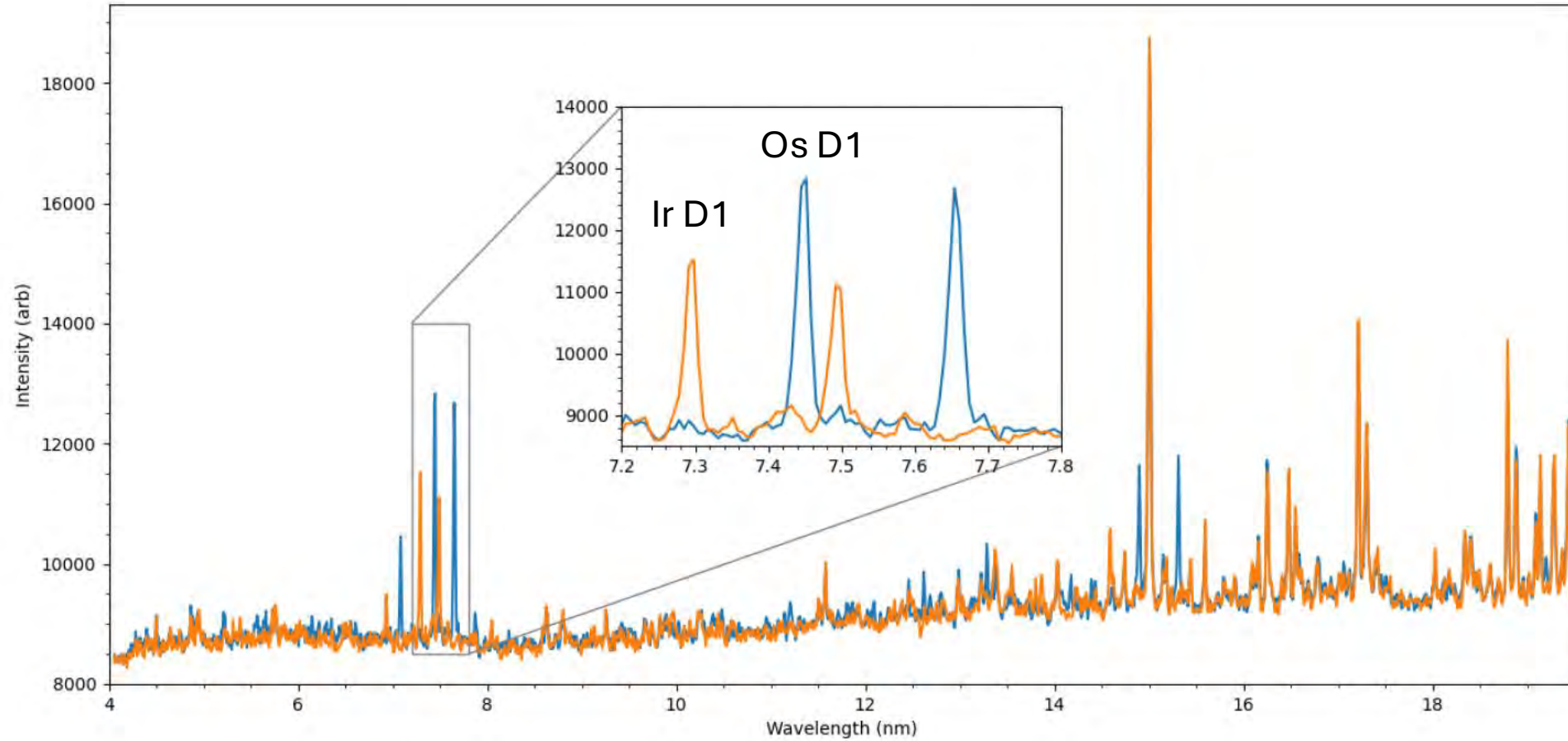
$$\delta E_{AB} = S_B \delta R_B$$

nuclear sensitivity coefficient

$$\delta R_B \equiv R_B - R_{B_0}$$



Ir ÉS Os 18 keV ELEKRONNYALÁB ENERGIÁN



EUV spectra of Na-like D1 $3s^2 S_{1/2} - 3p^2 P_{1/2}$ and Mg-like $3s^2^1 S_0 - 3s3p^3 P_1$ transitions for both Os and Ir, in orange and blue respectively.

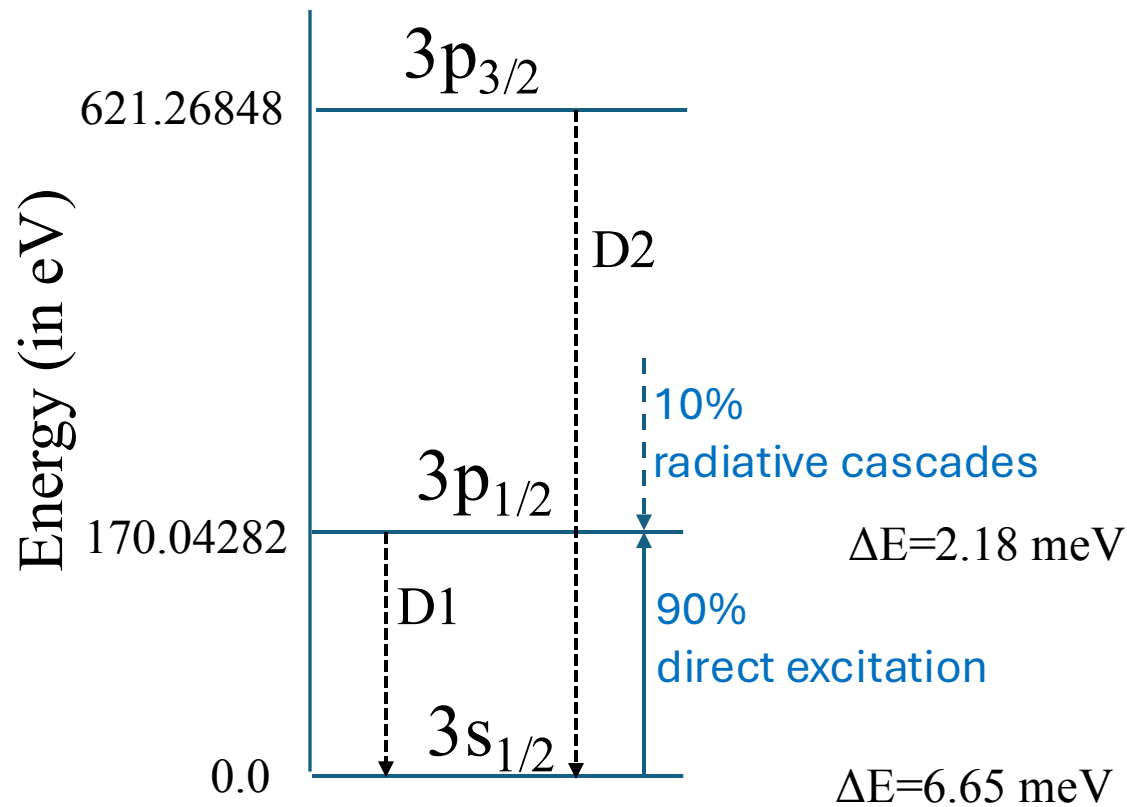
NÁTRIUMSZERŰ ENERGIASZINTEK POPULÁCIÓJA

Os-184	0.02(1) %	Ir-191	37.3(2) %
Os-186	1.59(3) %	Ir-193	62.7(2) %
Os-187	1.96(2) %		
Os-188	13.24(8) %		
Os-189	16.15(5) %		
Os-190	26.26(2) %		
Os-192	40.78(19) %		

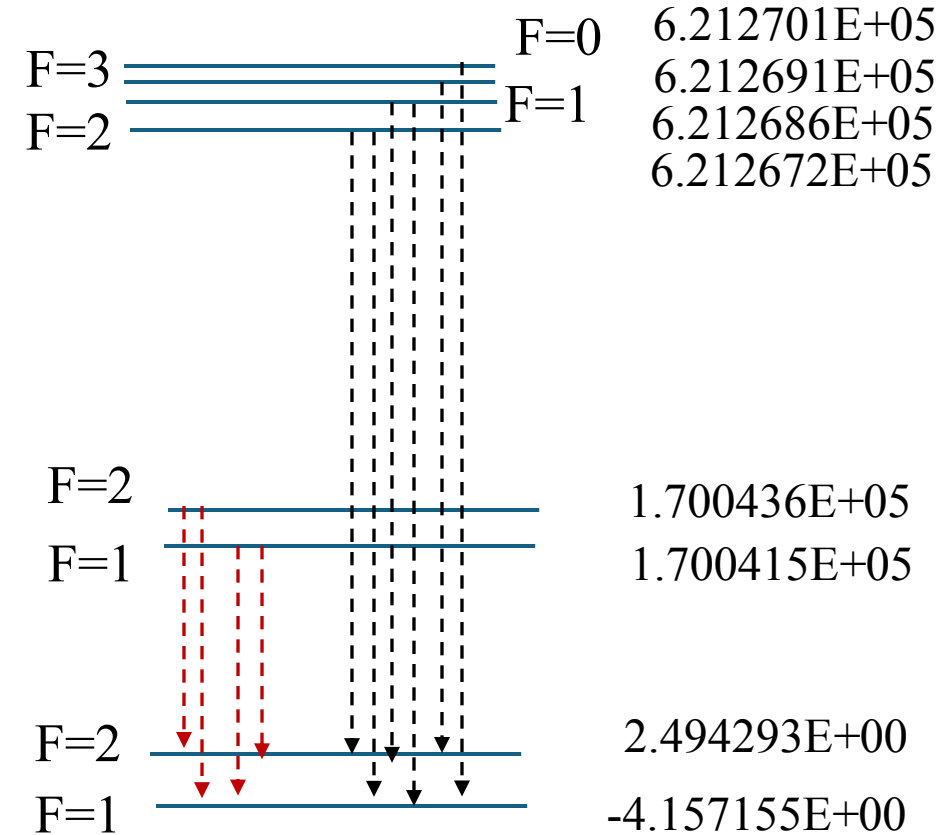
- ✓ The Ir and Os in the measurements have the natural abundance of their isotopes.
- ✓ Isotope with odd number of nucleons exhibit HF structure.

$$\Delta E = \frac{A}{2} K + \frac{B}{4} \frac{1.5K(K+1) - 2I(I+1)J(J+1)}{I(2I-1)J(2J-1)}$$

Energy (in meV)

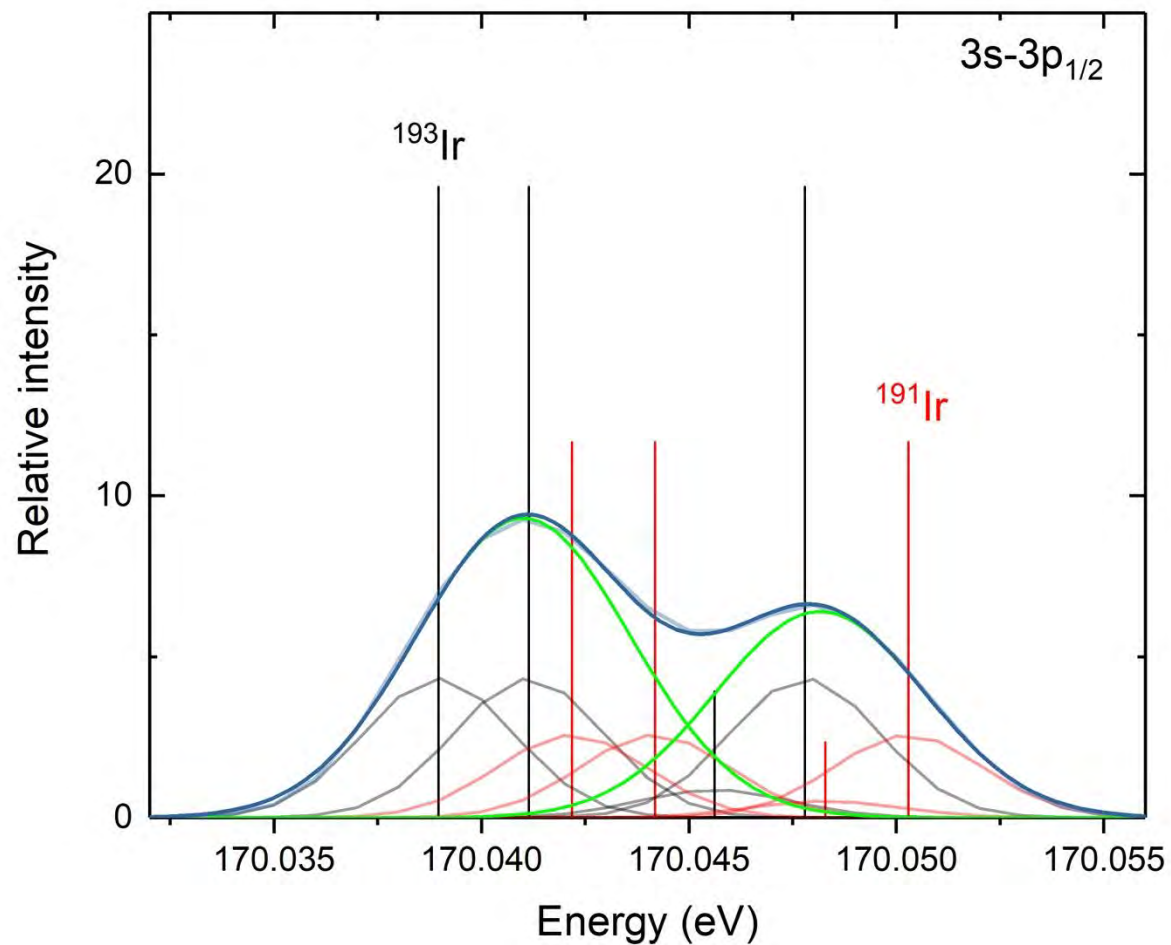


Fine-structure splitting

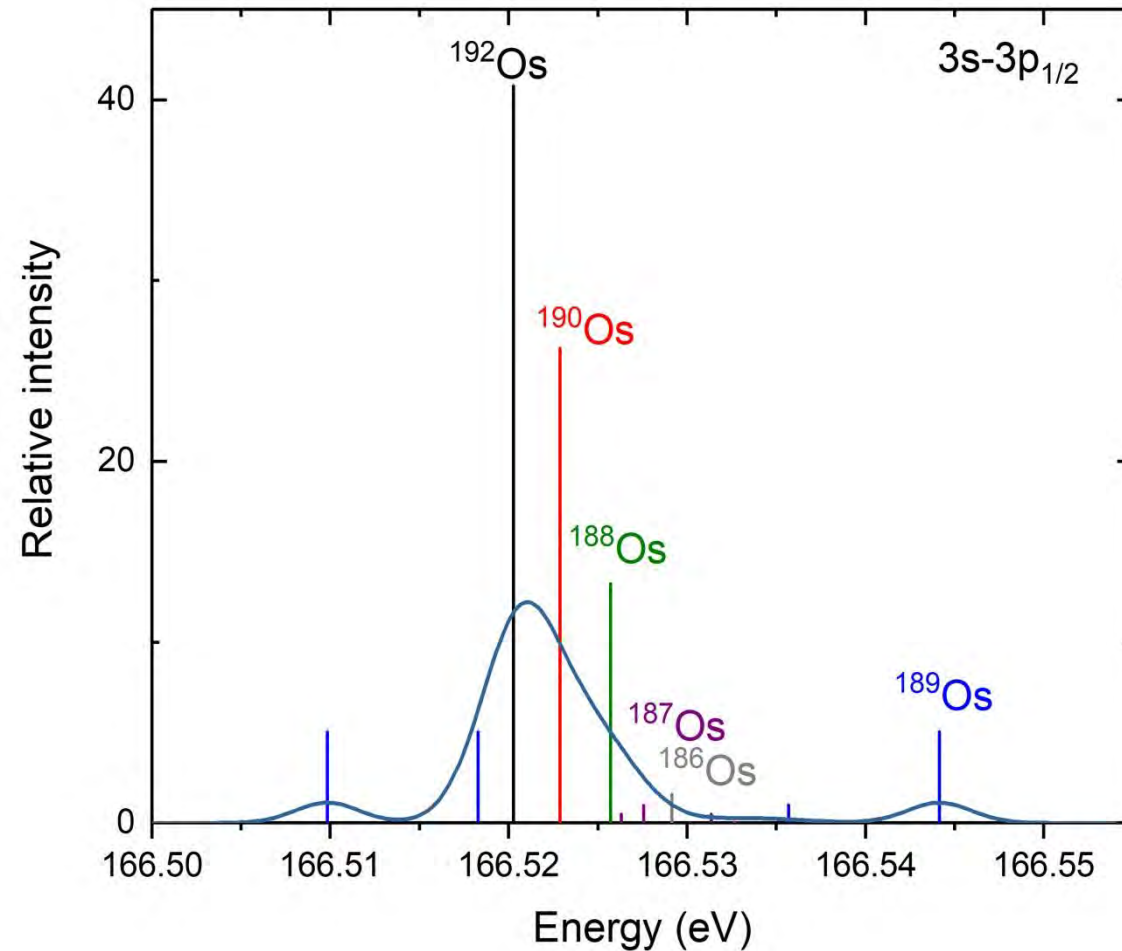


Hyperfine-structure splitting

HIPERFINOM SZERKEZET



HF splitting ~ 9 meV



HF splitting ~ 35 meV

Instrument resolution ~ 440 meV

EREDMÉNYEK: ^{191}Ir ATOMMAG TÖLTÉSSUGARA

Hosier et al., Physical Review Research, (2025) In print

5.4307(77) fm

Units: eV			
	Os D1 [eV]	Ir D1 [eV]	Ir-Os D1 [eV] (interpolation)
R(rms):	5.4064 fm	5.4000 fm	
DF	167.470 (0)	171.025 (0)	3.5550 (0)
B(1)	4.746 (0)	4.977 (0)	0.2310 (0)
B(RPA)	-0.118 (0)	-0.122 (0)	-0.0045 (0)
BB(RPA)	-0.011 (0)	-0.012 (0)	-0.0007 (0)
Ret(1)	0.016 (0)	0.020 (0)	0.0045 (0)
Ret(RPA)	0.004 (0)	0.004 (0)	0.0003 (0)
Ret(other)	0.000 (11)	0.0000 (11)	0.0000 (3)
CC(2)	-0.300 (0)	-0.303 (0)	-0.0032 (0)
BC(2)	-0.053 (0)	-0.055 (0)	-0.0019 (0)
BB(2)	0.011 (0)	0.011 (0)	-0.0001 (0)
GGG(3)	0.005 (0)	0.005 (0)	0.0001 (0)
Nuc. Rec.	-0.007 (2)	-0.007 (2)	0.0000 (0)
RMBPT(tot)	171.762 (11)	175.543 (11)	3.7805 (3)
SE(val)	-6.387 (0)	-6.725 (0)	-0.3375 (0)
Uehl(val)	1.162 (0)	1.245 (0)	0.0825 (0)
WK(val)	-0.045 (4)	-0.049 (4)	-0.0041 (4)
SE(val-x)	0.090 (1)	0.094 (1)	0.0041 (1)
VP(val-x)	-0.016 (0)	-0.017 (0)	-0.0010 (0)
SE(core)	-0.153 (2)	-0.161 (2)	-0.0072 (1)
VP(core)	0.027 (0)	0.029 (0)	0.0017 (0)
Other(vert)	0.000 (10)	0.000 (11)	0.0000 (5)
2-loop	0.019 (7)	0.020 (7)	0.0013 (5)
QED(tot)	-5.304 (13)	-5.564 (14)	-0.2602 (8)
TOTAL	166.458 (17)	169.979 (18)	3.5204 (8)
	(38)	(40)	(18)
	(25)	(27)	(12)
TOTAL [no BB(2)]	166.447 (17)	169.968 (18)	3.5205 (8)

$$\delta R_{\text{Ir}} = \frac{1}{S_{\text{Ir}}} [\delta E_{\text{Ir-Os}}^{\text{exp}} - (E_{\text{Ir}}^{\text{th}}(R_{\text{Ir}}) - E_{\text{Os}}^{\text{th}}(R_{\text{Os}}))]$$

key theoretical

Uncertainty

$$\Delta(\delta R_{\text{Ir}}) = \left[\frac{(S_{\text{Os}} \Delta R_{\text{Os}})^2}{S_{\text{Ir}}^2} + \frac{(\Delta[E_{\text{Os}}(R_{\text{Os},0}) - E_{\text{Ir}}(R_{\text{Ir},0})])^2}{S_{\text{Ir}}^2} \right. \\ \left. + \frac{(\Delta E_{\text{Os-Ir}}^{\text{M}})^2}{S_{\text{Ir}}^2} + (\delta R_{\text{Ir}})^2 \left(\frac{\Delta S_{\text{Ir}}}{S_{\text{Ir}}} \right)^2 \right]^{1/2}$$

experimental

Nuclear model dependence

$$\rho(r, \theta, \phi) = \frac{\rho_0}{1 + \exp[(r - c_{\text{def}})/a]} \quad c_{\text{def}}(\theta, \phi) = c[1 + \beta_2 Y_{20}(\theta, \phi)]$$

$$\delta E(R, \beta_2, t) = \delta R \frac{\partial E}{\partial R} + \delta \beta_2 \frac{\partial E}{\partial \beta_2} + \delta t \frac{\partial E}{\partial t} \\ \equiv S \delta R + S_{\beta_2} \delta \beta_2 + S_t \delta t$$

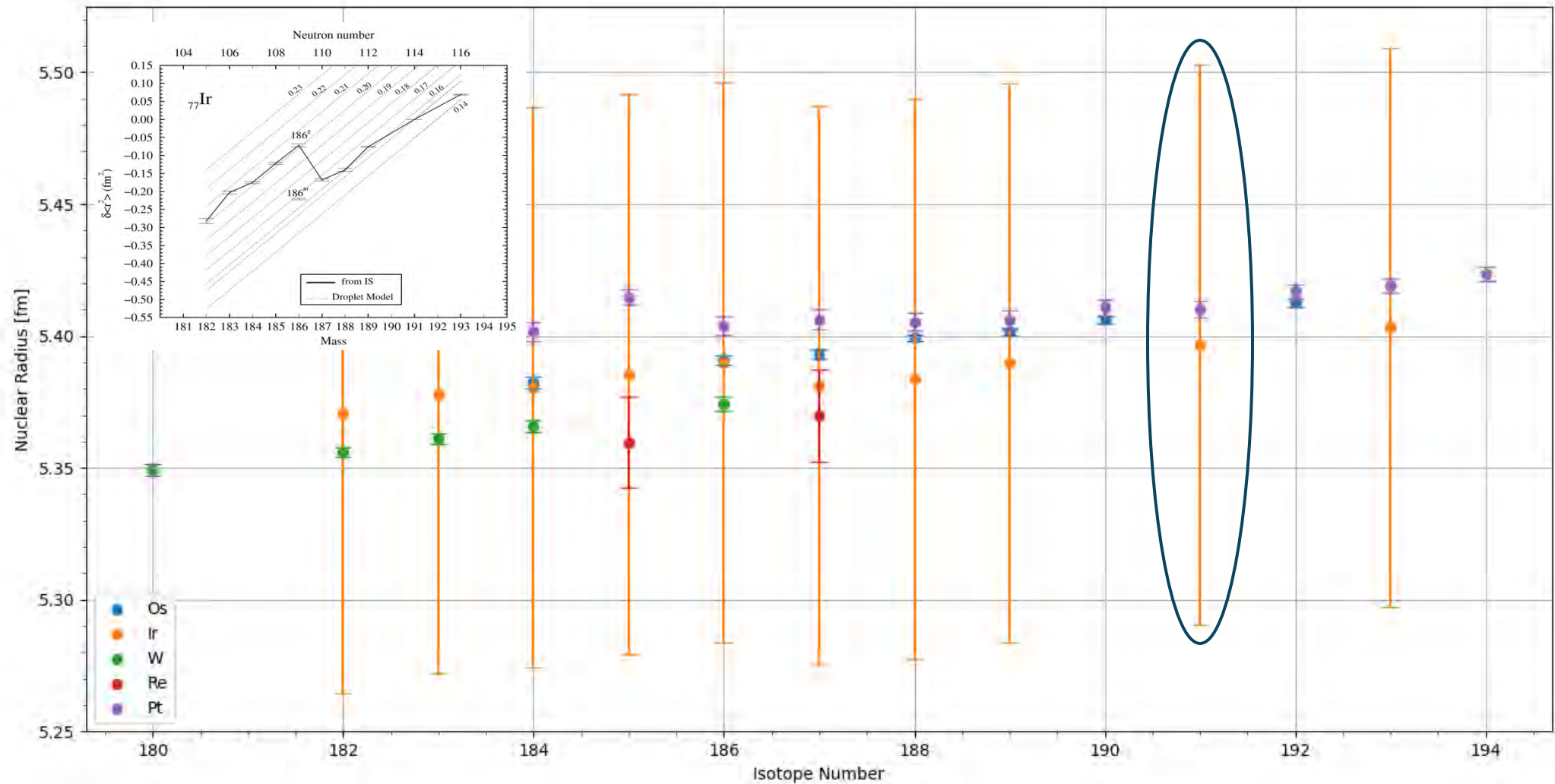
	units	Na-like D_1
S	eV fm ⁻¹	-0.4557
S_{β_2}	eV	0.0032
S_t	eV fm ⁻¹	0.0025
S_2	eV fm ⁻²	-0.026
$\Delta \beta_2$		0.17
Δt	fm	0.1
δR_{Ir}	fm	0.04
$\Delta S/S$		0.5%

Included in ΔS

$$(\Delta S/S) \delta R_{\text{Ir}} \approx 0.0016 \text{ fm}$$

EREDMÉNYEK: Ir ATOMMAGOK TÖLTÉSSUGARA

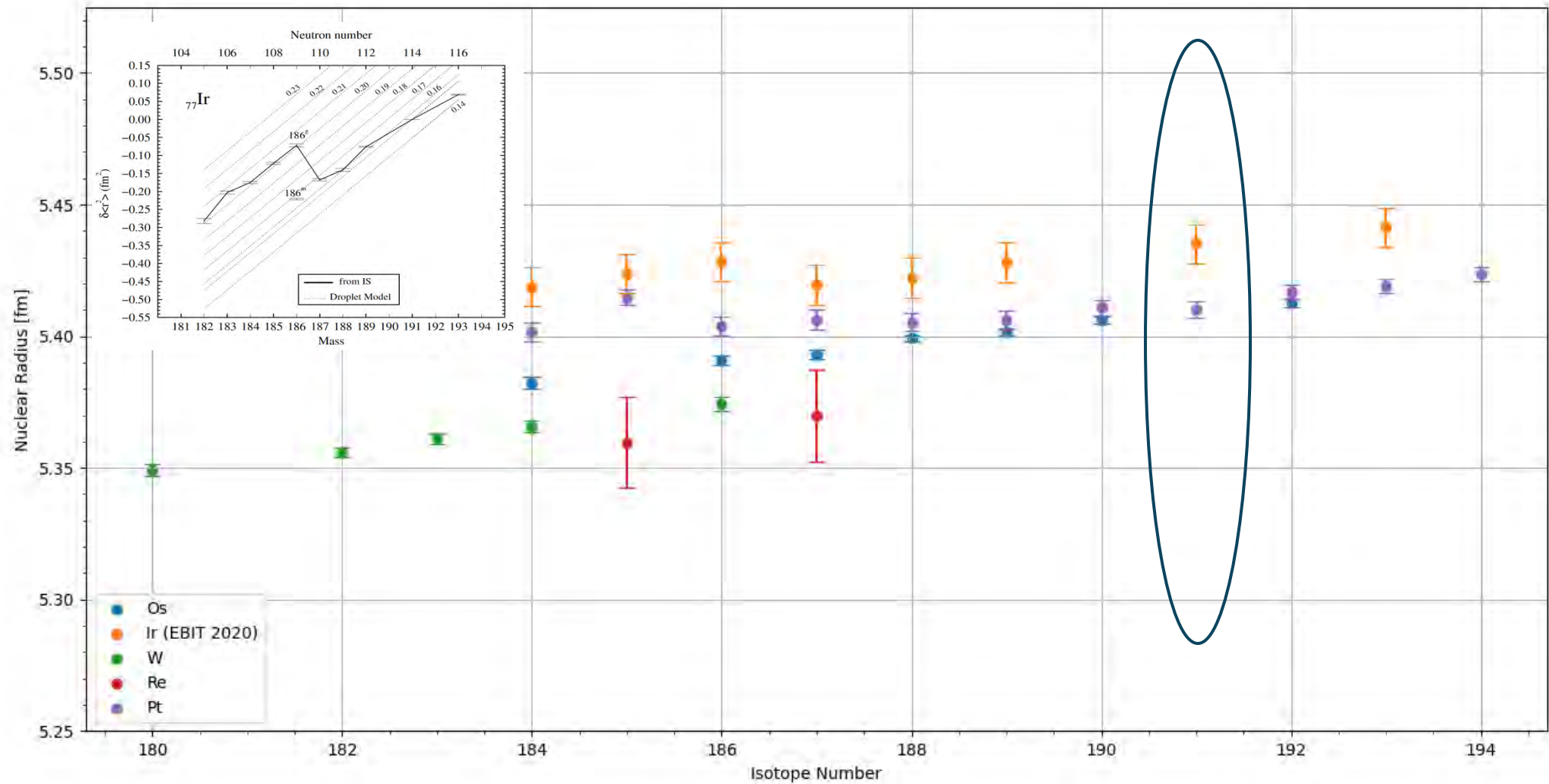
Hosier et al., Physical Review Research, (2025) In print



Angeli and K. P. Marinova, At. Data Nucl. Data Tables **99**, 69 (2013)

EREDMÉNYEK: Ir ATOMMAGOK TÖLTÉSSUGARA

Hosier et al., Physical Review Research, (2025) In print

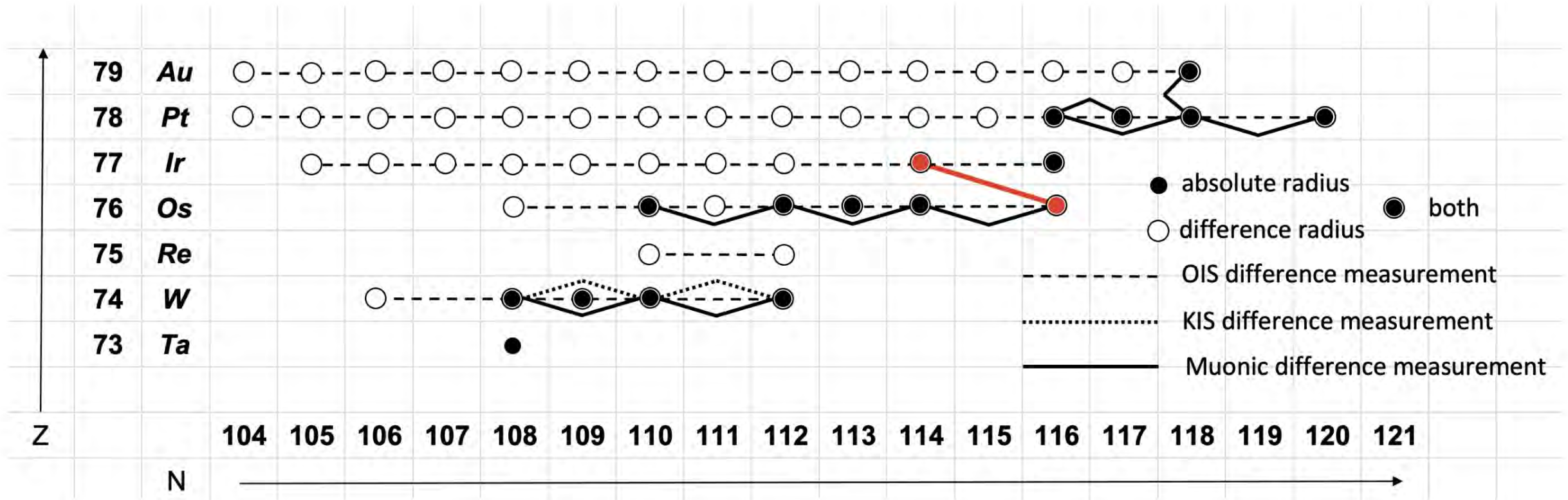


Our measurements combined with optical isotope shift data

ELEMEK KÖZÖTTI KÉNYSZERFELTÉTEL A MAGSUGÁR FELÜLETEN

wings (secondary)

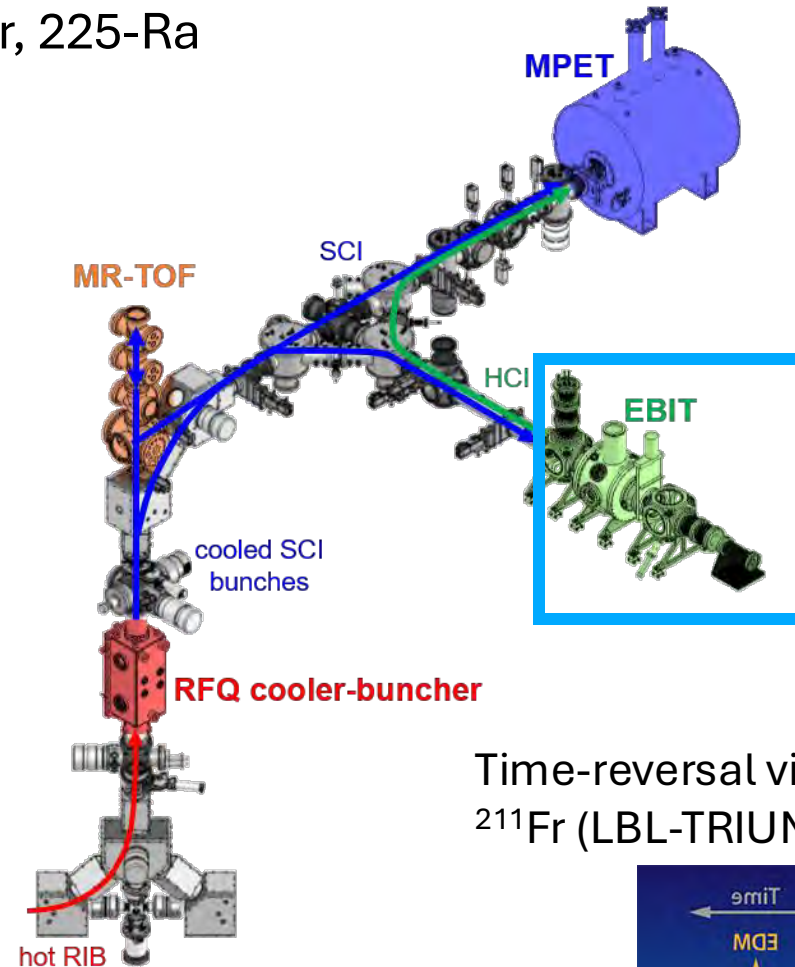
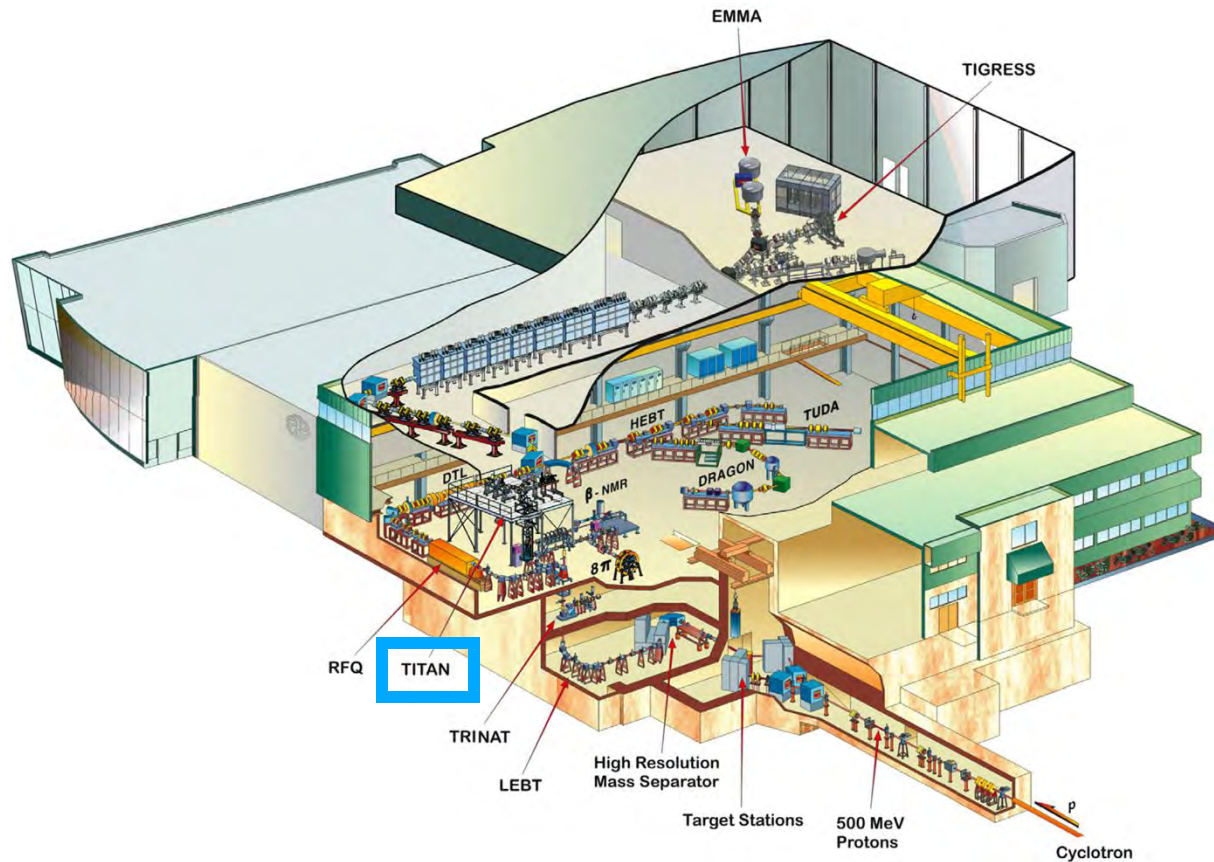
backbone (primary)



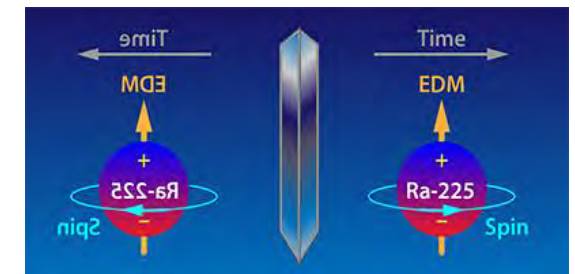
— Na-like ion Ir-Os measurement

JÖVŐ: TRIUMF's Ion Trap for Atomic and Nuclear Science (TITAN), Vancouver, Canada

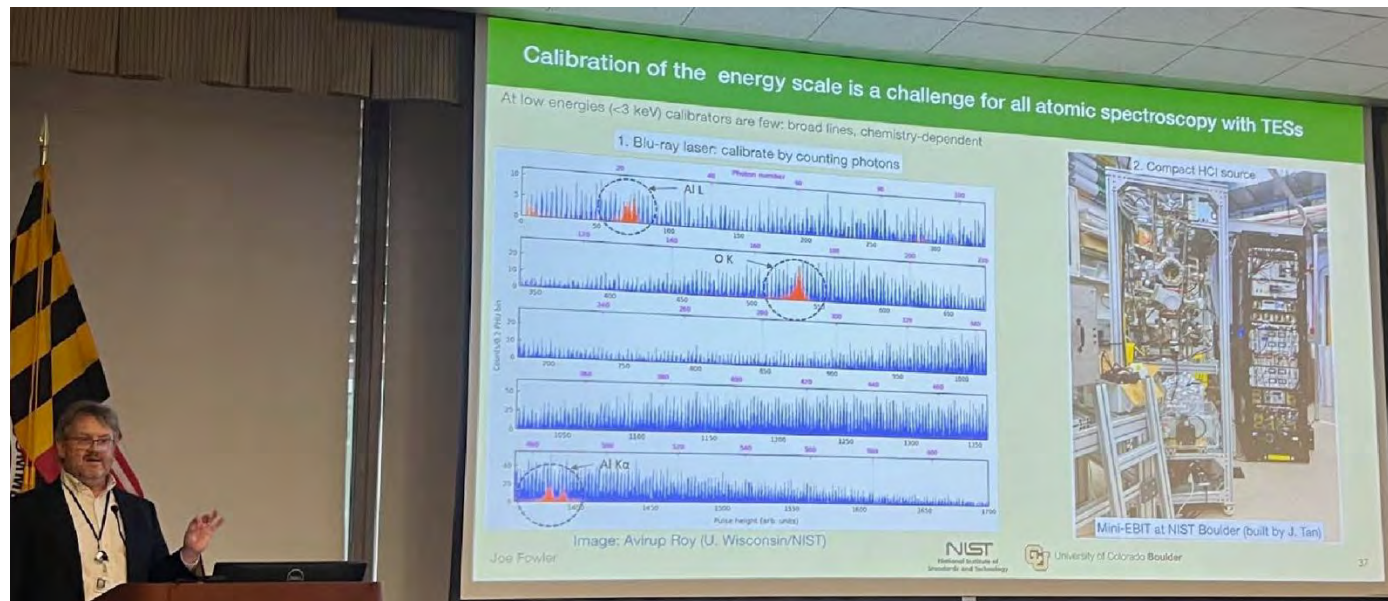
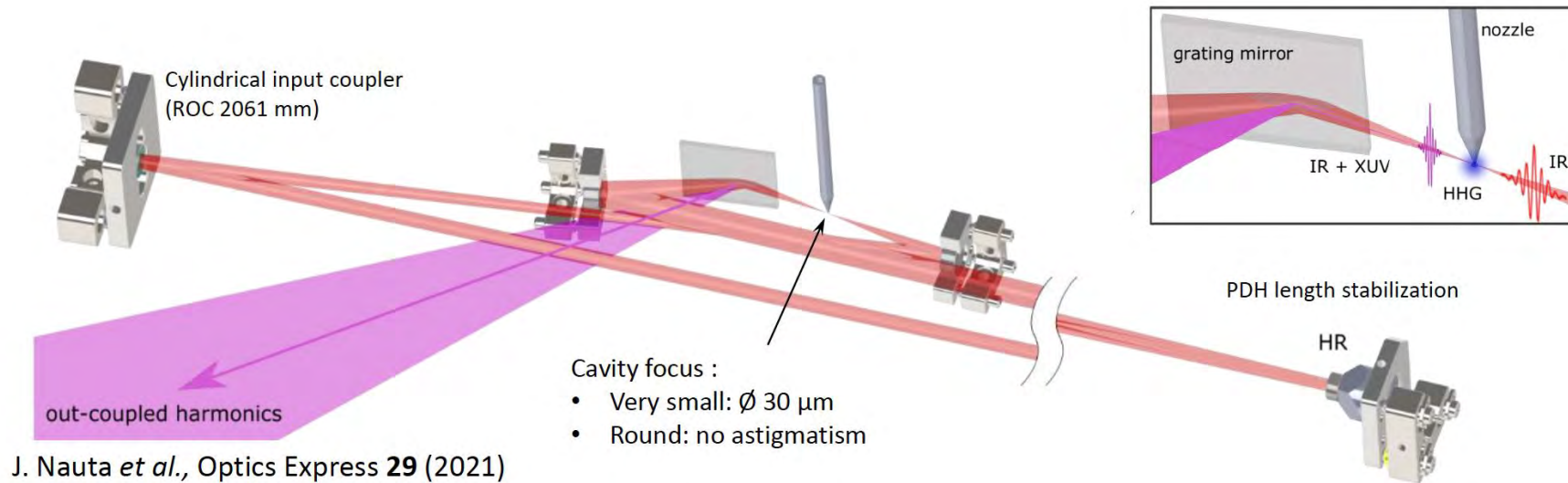
Fr, ²²⁵Ra



Time-reversal violation measurements:
²¹¹Fr (LBL-TRIUMF), ²²⁵Ra (Argonne NL)



JÖVŐ: XUV Frequency Combs, microcalorimeter



A jövő napfényes! Köszönöm!
 etakacs@clemson.edu